Geophys. J. Int. (2001) **147,** 499–516

Faulting and earthquake triggering during the 1783 Calabria seismic sequence

E. Jacques,[1,*] C. Monaco,[2] P. Tapponnier,[1] L. Tortorici[2] and T. Winter[3]

[1] *Laboratoire de Tectonique et Mécanique de la Lithosphère UMR CNRS* 7578, *Institut de Physique du Globe de Paris, France. E-mails: Jacques@ipgp.jussieu.fr; tappon@ipgp.jussieu.fr*

[2] *Istituto di Geologia e Geofisica, Università di Catania, Italy. E-mails: cmonaco@mbox.unict.it; tortoric@mbox.unict.it*

[3] *Bureau de Recherche Géologique et Minière, Orléans, France*

Accepted 2001 May 17. Received 2001 April 19; in original form 1999 March 26

SUMMARY

Between the 1783 February 5 and 1783 March 28, five earthquakes struck the southern part of Calabria. The main shock (February 5) and the first aftershock (February 6) devastated the region ENE of the Messina Strait. The greatest damage occurred along the foot of the Aspromonte Mountains south of San Giorgio Morgeto, and along the Tyrrhenian coast south of Palmi. A surface break about 18 km long, with several feet of downthrow to the west, formed along the Cittanova (Santa Cristina) Fault as a result of the main shock. On February 7, a third large shock ruined villages at the foot of the Serre Mountains north of San Giorgio Morgeto. Morphological and structural evidence, combined with a reassessment of observations made at the time of the earthquakes, suggest that these three shocks were shallow ($\leq$20 km) and related to slip on the west-dipping, NE-striking Cittanova–Sant'Eufemia, Palmi–Scilla and Serre normal faults, respectively, which juxtapose the basement of the Aspromonte and Serre mountains with the Pleistocene deposits of the Gioia Tauro and Mesima basins, and border the Palmi coastal high. The three faults belong to an active rift that stretches from northern Calabria to offshore the Ionian coast of Sicily. The spatial coupling between the 1783 events is investigated by resolving changes of Coulomb failure stress. The main shock (1783 February 5, $M \sim 7$), on the Cittanova and Sant'Eufemia faults, increased that stress by several bars on the Scilla Fault, triggering the 1783 February 6 earthquake ($M \sim 6.5$). The cumulative effect of these two shocks was to raise the Coulomb stress by more than 1 bar on the SW part of the Serre Fault, which was subsequently the site of the 1783 February 7 shock ($M \sim 6.5$). In turn, the first three events increased the stress by about 1 bar on the NE part of this latter fault, leading to the 1783 March 1 shock ($M \sim 5.7$). The gap between the 1783 February 7 and 1783 March 1 events may be related to the previous occurrence of an earthquake 124 yr before (1659 November 5, $M \sim 6$), which had already released stress locally. The occurrence of the last 1783 event (28 March) is not as simply accounted for by Coulomb modelling, in part because it remains unclear which fault slipped and how deep this event was. Overall, the 1783 sequence increased the Coulomb failure stress by several bars south of the Messina Strait and north of the epicentral region of the 1693 SE Sicily (Catania–Noto) earthquakes. 125 yr later, this same region was the site of the 1908 Messina earthquake, also a normal faulting event. Our study thus provides one convincing example in which Coulomb stress modelling brings insight into the spatial dynamics of seismic sequences.

Key words: crustal deformation, earthquakes, Italy, normal faulting, stress distribution.

* Now at: Equipe de Tectonique active et Paléosismologie, UMR CNRS 7516, Institut de Physique du Globe de Strasbourg, France. E-mail: Eric.Jacques@eost.u-strasbg.fr

INTRODUCTION

The Quaternary tectonics of the southern tip of Italy (Fig. 1) are dominated by normal faulting (e.g. Tapponnier 1977; Tapponnier *et al.* 1987; Westaway 1993; Tortorici *et al.* 1995; Monaco *et al.* 1995, 1997). Normal faults follow the Tyrrhenian side of Calabria and continue, across the Strait of Messina, along the Ionian coast of Sicily forming the 'Siculo-Calabrian

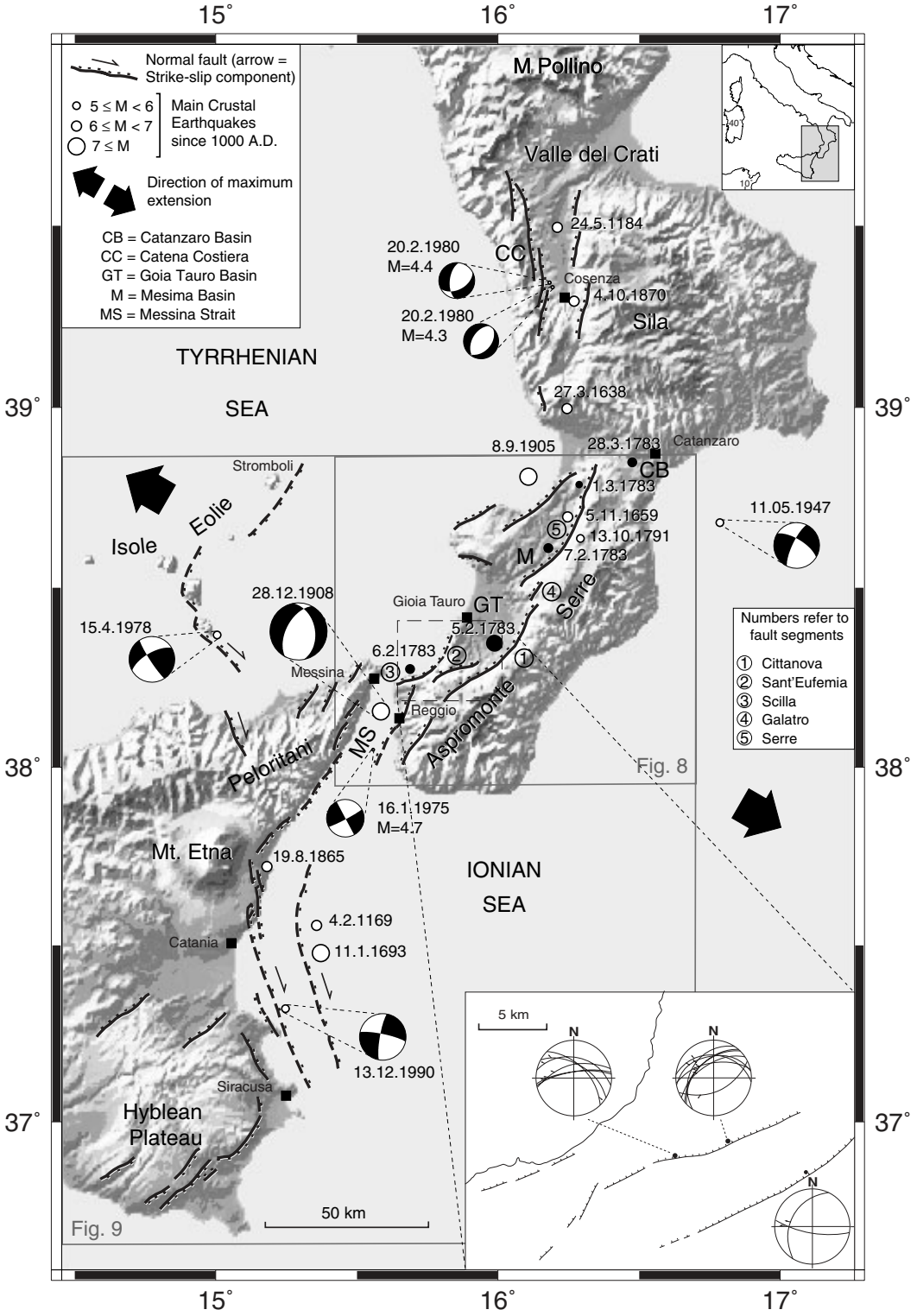

Figure 1. Seismotectonic map of the Calabrian Arc and eastern Sicily. Faults are mainly normal (barbs on downthrown block) and Pleistocene–Holocene in age. Crustal seismicity ($H < 35$ km) since 1000 AD (Postpischl 1985; Boschi *et al.* 1995) and focal mechanisms of instrumental earthquakes (Gasparini *et al.* 1982; Cello *et al.* 1982; Anderson & Jackson 1987; Amato *et al.* 1995) are shown. Numbers refer to fault segments: 1, Cittanova; 2, Sant'Eufemia; 3, Scilla; 4, Galatro; 5, Serre. The events of the 1783 earthquake sequence are represented as black dots. Boxes indicate the locations of Figs 8 and 9. Inset shows kinematic slip indicators on fault segments 1 and 2.

rift zone' (Monaco *et al.* 1997). Several of the faults cut and offset Upper Pleistocene to Holocene sediments along escarpments with young morphology, which bound steep range fronts (Catena costiera, Aspromonte, Serre, Peloritani). The high level of crustal seismicity is attested by numerous instrumental and historical earthquakes since 1000 AD. (Postpischl 1985; Boschi *et al.* 1995) with magnitudes of up to 7.1 and intensities of up to XI–XII MCS. Tectonic studies (e.g. Tapponnier *et al.* 1987; Mazzuoli *et al.* 1995; Tortorici *et al.* 1995; Monaco *et al.* 1995, 1997) and fault plane solutions (Gasparini *et al.* 1982; Cello *et al.* 1982; Anderson & Jackson 1987) show that, overall, the direction of extension along the Quaternary Siculo-Calabrian rift zone is roughly ESE–WNW.

In 1783, the southern part of Calabria was struck by one of the most devastating earthquake sequences in Western Europe. Five large shocks occurred along a zone about 100 km long in less than two months. In this paper, we first identify the faults that ruptured during the earthquakes. For this, we combine a reassessment of the available historical information with geological and geomorphological field evidence supported by the analysis of 1:33 000 scale aerial photographs and SPOT satellite images. After elucidating the pattern of interacting fault segments that broke, we try to understand the spatial coupling between the events of the sequence by resolving the changes of Coulomb failure stress caused by each earthquake rupture using a simple dislocation model in an elastic half-space (King *et al.* 1994). In doing this, we follow studies performed in California (e.g. Reasenberg & Simpson 1992; Stein *et al.* 1992; King *et al.* 1994), in Afar (Jacques 1995; Jacques *et al.* 1996) and in the Apennines (Nostro *et al.* 1997) that have shown that modelling Coulomb failure stress changes induced by one or more events can clarify the distribution of future events. The stress changes are calculated on faults with given strikes, or on optimally oriented faults, given the regional stress field. We finally broaden the regional scope of our study by including in the modelling all the large earthquakes that have occurred in eastern Sicily and southern Calabria over the last 350 yr.

GEOLOGICAL AND STRUCTURAL FRAMEWORK OF SOUTHWESTERN CALABRIA

The Aspromonte and Serre mountains (maximum elevation 1956 m at Montalto) form the structural backbone of SW Calabria. They are composed of uplifted metamorphic basement (chiefly gneisses and granites). The basement is a pile of several thrust sheets, involving Cretaceous sediments in the eastern, external part (e.g. Ogniben 1973). The mountains slope rather gently towards the Ionian Sea to the east, but their western edge is steeper and controlled by normal faults. The faults dip west and bound a major Plio-Pleistocene trough (Gioia Tauro and Mesima basins) (Fig. 2). The southern part of the Gioia Basin is separated from the Tyrrhenian Sea by the Palmi high (maximum elevation 593 m), along which basement identical to that in the Aspromonte has been uplifted and tilted by movement on another west-dipping, offshore normal fault (Figs 2a and b). On this high, the basement is unconformably covered by patches of calcareous sandstones and white marls of Tortonian to Early Pliocene age (Figs 2a and b). The Gioia Basin is filled by about 600 m of Plio-Pleistocene marine sediments (Fig. 2b). The basal deposits, visible near Sant'Eufemia and San Giorgio Morgeto, are cross-bedded sands and calcarenites with conglomeratic lenses of Late Pliocene–Early Pleistocene age ($\approx$2 Ma), about 70 m thick (beach deposits, Fig. 2a). They are overlain by a clay and silt sequence several hundred metres thick. Pumice-rich horizons are found in the upper part of the sequence. Bathyal and circalitoral microfaunal assemblages imply that, as for the analogous sequence found south of Villa San Giovanni (Barrier 1987), the clays were deposited between the Early and Middle Pleistocene (1.8–0.5 Ma) in water depths of around 400 m. In much of the Gioia Basin, 70 m cross-bedded beach sands cap, with slight angular unconformity, the marine sequence. These sands onlap the basement in the Delianova area (Fig. 2a). Near Molocchio and Oppido Mamertina, coarser conglomeratic lenses interfinger with the sands, implying synsedimentary tectonic activity along the edge of the Aspromonte (Fig. 2b). The upper beach sands extend laterally to the Tyrrhenian coastal deposits, in which the typical Strombus Bubonius fauna is found (Bonfiglio & Berdar 1986). Given the probable westward progradation of these deposits and westward migration of the coastline, however, the age of the upper beach sands in the Gioia Basin may only be estimated to be between the upper Middle Pleistocene (200 ka) and the Late Pleistocene (100 ka). Middle to Late Pleistocene deposits are also found south of Villa San Giovanni (Dumas *et al.* 1979; Barrier & Keraudren 1983; Barrier 1987) (Fig. 2a), but with a different facies (Gilbert-type fan delta conglomerates). Between Villa San Giovanni and Gioia Tauro, as many as nine to 10 levels of Pleistocene marine terraces step up to about 600 m on the Palmi–Bagnara coastal high (Gignoux 1913; Dumas *et al.* 1980, 1982; Ghisetti 1981) (Fig. 2a), attesting to sustained recent uplift of this high relative to sea level.

The uppermost deposits in the Gioia Basin are continental alluvial fanglomerates and sands, which cover unconformably the Mid–Upper Pleistocene (200–100 ka) beach sands; Lower Pleistocene deposits of similar facies cap directly the basement on top of the flat Aspromonte planation surface ('Piani') at elevations of 1000 m or more (Fig. 2).

Such stratigraphic and structural observations are in keeping with the generally accepted tectonic evolution of the inner, Tyrrhenian part of the southern Calabrian Apennines (e.g. Boccaletti *et al.* 1974; Tapponnier 1977; Ghisetti & Vezzani 1982; Rehault *et al.* 1984; Malinverno & Ryan 1986; Dewey *et al.* 1989). Here, much of the SE-directed overthrusting induced by the subduction of the African–Apulian Plate under the growing Tyrrhenian Plate stopped after the Tortonian. In the outer, Ionian part of the belt, such overthrusting continued into the Pleistocene, but, after the late Pliocene, the Tyrrhenian side of the Aspromonte was affected by extensional faulting (Tortorici *et al.* 1995; Monaco *et al.* 1996). The Gioia and Mesima basins developed on the blocks tilted southeastwards by such faulting during the Pleistocene.

THE 1783 EARTHQUAKE SEQUENCE

From the beginning of February until the end of March 1783, five large earthquakes devastated the southern part of Calabria between Reggio di Calabria and Catanzaro (Fig. 3). This remarkable sequence started with a catastrophic event at 12:45 local time on February 5 1783. Towns and villages located at the western foot of the northern Aspromonte, such as Cittanova (at the time Casalnuovo) Molochio, Oppido Mamertina,

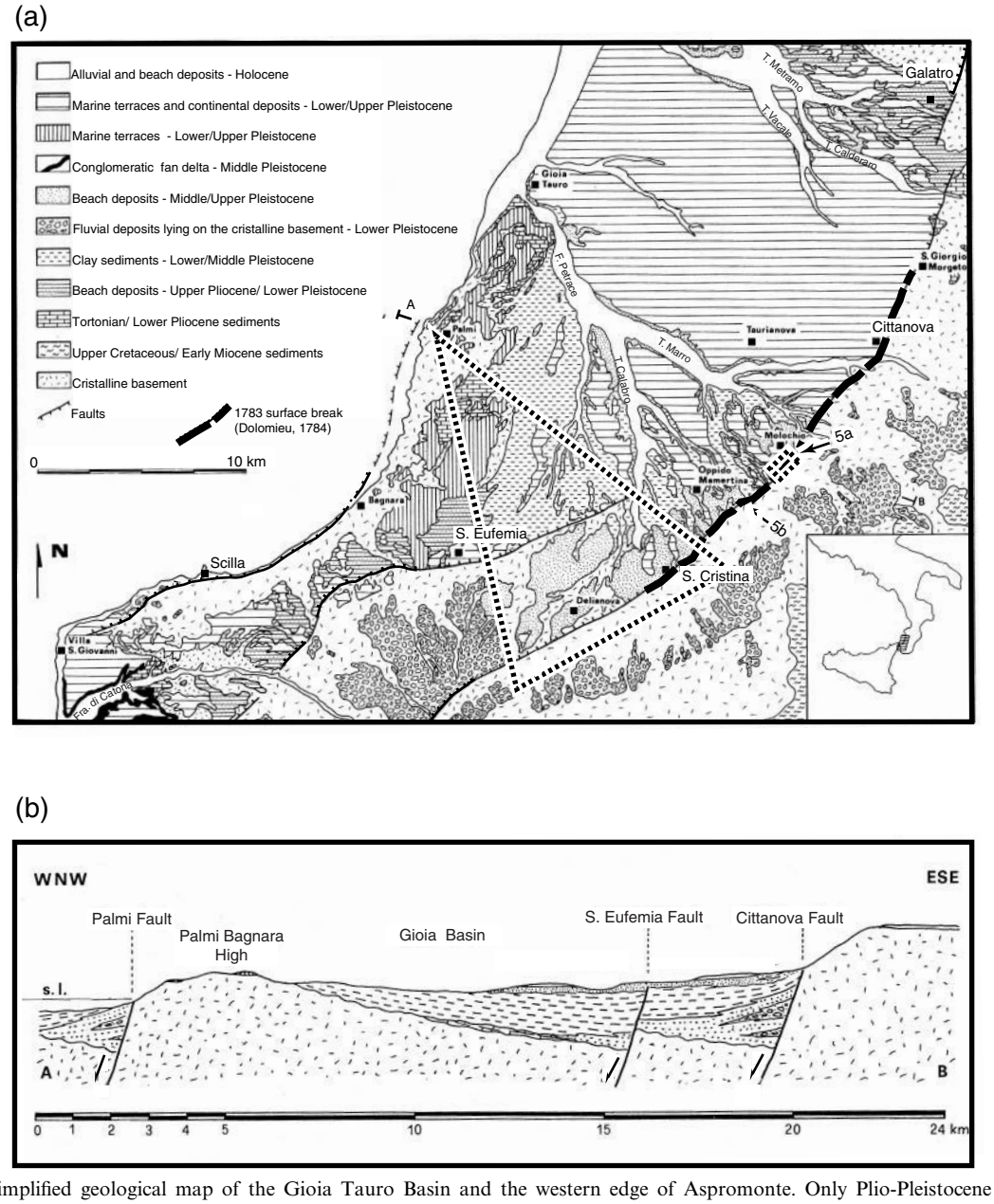

Figure 2. (a) Simplified geological map of the Gioia Tauro Basin and the western edge of Aspromonte. Only Plio-Pleistocene formations are represented in detail. The Galatro, Cittanova (Santa Cristina) and Sant'Eufemia faults bring uplifted metamorphic basement against Pleistocene terrigenous deposits. Another fault (the Scilla Fault) is responsible for basement uplift along the Palmi coastal high and sea cliff. View angle and locations of Figs 5 and 7 are outlined by boxes. (b) Schematic cross-section along profile A–B in (a), no vertical exaggeration.

Terranova and Santa Cristina, were completely destroyed. This event also caused important damage in cities closer to the Tyrrhenian coast (Palmi, Bagnara and Scilla) (Figs 2 and 3). The area between Molochio and Santa Cristina was the site of spectacular landslides that dammed valleys and created many lakes (Vivenzio 1783; Hamilton 1783; Dolomieu 1784; Baratta 1901; Cotecchia *et al*. 1969).

On February 6 1783 at 01:06, a second large shock struck mostly the coastal area between Scilla and Palmi, bringing the cumulative damage in this area to a level almost comparable to that in the Aspromonte piedmont. Major rockslides along the cliff west of Scilla (part of Monte Paci and Campallà fell into the sea) and a tidal wave (Fig. 3) that principally affected the town of Scilla and the lowland of Punta Faro (on Capo Peloro, Sicily's northeasternmost cape) were triggered by the second earthquake. Although Dolomieu (1784) and Baratta (1901), among others, disagree on whether the wave was a mere consequence of the rockslide or a small, earthquake-generated tsunami, most chroniclers concur in locating the 'centre' of this second shock offshore, not far from Scilla (Fig. 3).

On February 7 (at about 20:00), a third shock ruined the small towns of Soriano (leading to the destruction of well-built edifices, for example, the Benedictine convent rebuilt after the 1659 earthquake, Dolomieu 1784), Sorianello, Gerocarne and Pizzoni, at the western foot of the Serre Mountains, about 40 km northeast of the epicentral area of the catastrophic February 5 event (Fig. 3) (Baratta 1901). Dolomieu (1784) notes that this earthquake increased significantly the damage

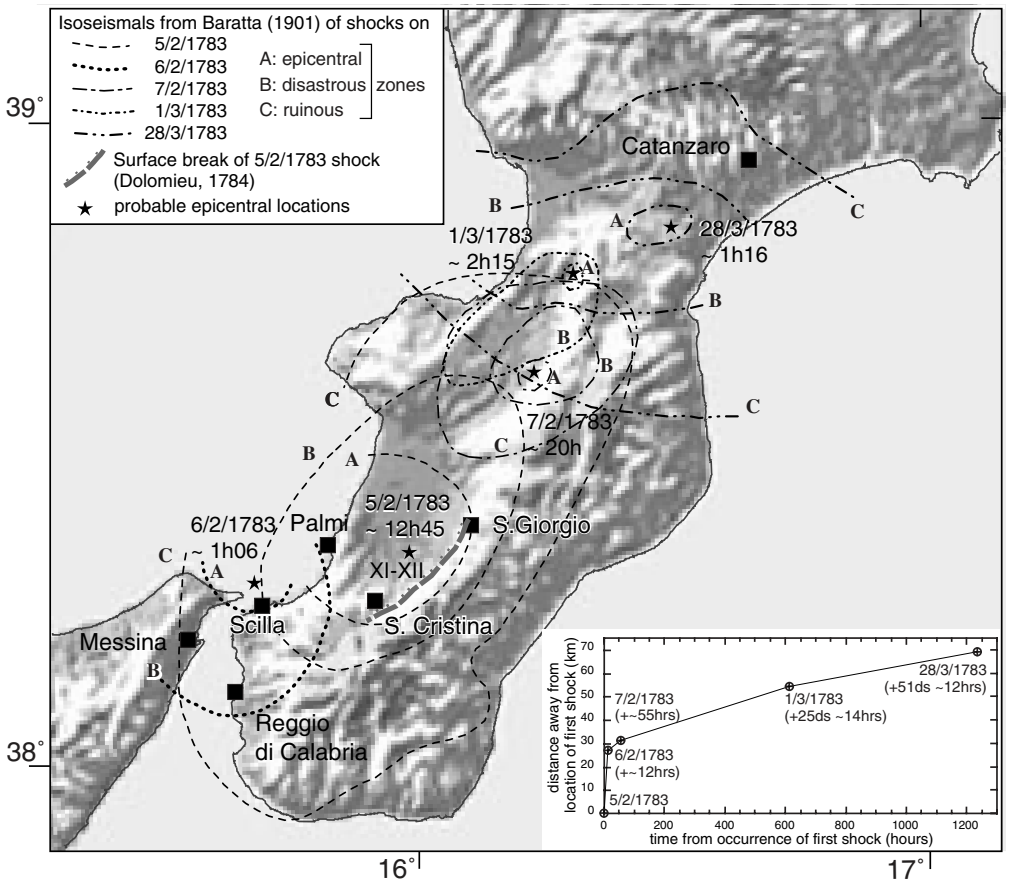

Figure 3. Mesoseismal areas of the five principal shocks of the 1783 earthquake sequence (after Baratta 1901). Stars correspond to probable epicentral locations. Curves corresponding to approximate limits of epicentral (A), disastrous (B) and ruinous (C) zones, as defined by Baratta, are shown. Inset shows distance away from location of first shock as a function of time from occurrence of first shock.

in cities such as San Giorgio Morgeto, situated in the north-eastern part of the epicentral area of the February 5 event, as did the shock of February 6 in the southwestern part of the area, near the Tyrrhenian coast.

On March 1 1783 (at about 02:15), a fourth shock struck an apparently smaller area near Polia (Baratta 1901), about 20 km north of the February 7 epicentre (Fig. 3). Finally, on March 28 (at about 01:16), still further northeast (Fig. 3), the fifth and last important shock of the sequence caused destruction in the towns of Borgia and Girifalco (Baratta 1901), closer to the Ionian sea.

In addition to the five major events described above, hundreds of smaller aftershocks were felt, particularly in the hours and days following the main February 5 event, and then with decreasing frequency until the end of 1783 (Baratta 1901). Baratta singles out one such aftershock, which brought significant additional damage, mostly to Messina, Reggio di Calabria and Scilla, in the evening of February 7 (at about 22:00), and thus probably had its epicentre located at the southwesternmost tip of the area strongly shaken by the main 1783 earthquakes.

Comparison and quantitative assessment of damage and mesoseismal effects due to the earthquakes

Among the five principal shocks, that on March 1 appears to have been the weakest, and there is overwhelming evidence that the first February 5 event was by far the strongest. All chroniclers agree that the greatest destruction occurred just west of the Aspromonte, in the Gioia Basin, and infer the 'centre' of this first and main shock to have been located under it, near Oppido and Molochio (e.g. Dolomieu 1784; Hamilton 1783; Baratta 1901). To the surprise of many, Reggio di Calabria and Messina were relatively undamaged (e.g. Hamilton 1783). Dolomieu (1784) suspected some of the destruction in Messina to have been related to the fact that many buildings there had been weakened by the large 1693 earthquake (Fig. 1) and other smaller shocks in the following 90 yr. Destruction in villages and small towns along the Ionian coast of Calabria was moderate compared to that on the Tyrrhenian side of the Aspromonte (Baratta 1901). Dolomieu (1784) and Hamilton (1783) stress the general fact that villages built on basement rocks in the Aspromonte Mountains (e.g. San Giorgio) suffered less than those built on the loosely consolidated alluvium of the 'plain' below. The particularly disastrous destruction in the plain was in part due to its peculiar morphology, characterized by tabular mesas of uplifted Pleistocene clays and sands incised by NW–SE river canyons up to 200 m deep and 1500 m wide (Fig. 2a). In the territories of Santa Cristina and Oppido, the steep edges of such valleys collapsed extensively. Both Hamilton (1783) and Dolomieu (1784), and more recently Cotecchia *et al.* (1969), describe how, on February 5, entire olive groves, cultivated flats or parts of villages on the mesas slid several hundred metres to up to a few kilometres down into the valleys. In several instances, to the bewilderment of all, the top surface

of these far-travelled slide-blocks remained mostly intact. On the flat mesas, numerous cracks were observed to run parallel to the edges of the canyons (e.g. Hamilton 1783). Compaction of the permeable sediments of the 'plain' was widespread and spectacular. Post-seismic elevation differences in the originally level surface of cultivated fields and uplift of masonry foundations relative to the ground surface reached up to 10 ft in places. Sand fountains spurted water to heights of several feet. The cones and craterlets left by such fountains were particularly abundant in the valleys of larger rivers such as Mammella, Metramo and Petrace (Hamilton 1783). All accounts indicate that only the main February 5 event produced such strong effects. Water flow in the Metramo was even reported to have stopped during the climax of this event, to resume stronger and muddier minutes later.

The ground shaking on February 5 was so strong that people in the fields were thrown down. Trees swung so hard that the tips of their branches touched the ground. Many were uprooted. Others had their trunks broken near the base (Dolomieu 1784). In Terranova, heavy pavement and foundation stones were found dislodged from their original emplacement and upturned (from Sarconi 1784, p.158 in Baratta 1901, p.272), an indication of particularly strong vertical acceleration. In much of its epicentral area the first shock was felt as a sudden, violent blast. Its great force must have been the main cause of the particularly thorough collapse of constructions. Although kilometric-scale landslides contributed largely to the destruction of Terranova and Molochio, they were a less important factor at Oppido and Casalnuovo (Hamilton 1783; Dolomieu 1784). These latter towns were nevertheless reduced to heaps of almost structureless ruins. Moreover, Casalnuovo had been built with particular care with wide streets and low-level houses after the earthquake of 1659 (Fig. 1) (Dolomieu 1784). Throughout the epicentral region of the main shock, numerous well-built edifices (e.g. convents, castles and palaces) were levelled to the ground (Hamilton 1783; Dolomieu 1784).

The total number of fatalities was in excess of 30 000. Official statistics differ by as much as 15 per cent, but fall short of the qualitative assessments made by either Dolomieu or Hamilton. While both estimated the earthquakes to have killed at least 40 000 people, Vivenzio (1783) calculated that number to be 35 160, and Baratta (1901) put it at 30 145. The accurate population records kept in towns and villages of the Kingdom of Naples, and the detailed report of damage and casualties prepared by the team of naturalists and engineers that the Royal Academy of Naples despatched to the site of the disaster permit one to make precise estimates of the loss of life at a local level. The map of Fig. 4 shows the percentages of inhabitants killed by the earthquakes in each village or city listed in Vivenzio's (1783) tables. The villages and towns where more than 300 people were killed, according to Baratta (1901) and his sources, are also listed in Table 1.

Although caution must be exercised in using such numbers to assess the effects of earthquakes, the map and the list lend quantitative support to the descriptions summarized earlier in this paper. With the exception of Messina and Borgia, all the localities listed in Table 1 belong to the zone outlined on Fig. 4 where fatality rates generally exceeded 15 per cent (Vivenzio 1783). Moreover, the 11 localities where the number of fatalities exceeded 900 belong to the central part of this zone. We infer this zone to correspond to the region of maximum intensity, at least for the first two shocks of the sequence, without drastic biases due to variations in construction style or site geology. The high fatality rates in Scilla appear to have resulted in part from the tidal wave caused by the second shock (e.g. Baratta 1901). In Bagnara, where there is no report of a tidal wave, they were perhaps in part due to the peculiar location of the city on a narrow alluvial delta between cliff and sea. Fatality rates were nearly as high, however, in Palmi and Seminara, where none of these circumstances prevailed (Vivenzio 1783). Biases related to differences in population density probably exist, but we also infer them to be small. The northeastern limit of the zone, for instance, which lies within the densely populated Calabrian plain, is fairly well defined. The southwestern limit, in the more sparsely inhabited Aspromonte Mountain, is less accurately defined. Nevertheless, fatality rates generally much smaller than 15 per cent throughout the region east of Villa San Giovanni and Reggio di Calabria and along the Ionian coast (Vivenzio 1783) indicate that intensities were much smaller along the southern and southeastern slopes of the Aspromonte than northwest of it. The very low fatality rates in three localities (Canolo: 2/1426 i; Antonimina: 20/830 i; Plati or Mottaplati: 25/1143 i) (Vivenzio 1783), situated only 5 km southeast of the crest of the Aspromonte and almost opposite Cittanova, Molochio and Santa Cristina (Fig. 4), imply not only that ground shaking intensities decreased dramatically across the Aspromonte, but also that the strike of the southeastern limit of the maximum intensity zone could not have been very different from that shown. The position chosen for this limit in Fig. 4 minimizes the surface of this zone. The relatively large number of fatalities in Messina, which is located outside the maximum intensity zone of Fig. 4, is probably mostly a consequence of its large population, in addition to the architectural weakening noted by Dolomieu. On the other hand, the low fatality rates north of Galatro (Fig. 4), in spite of the occurrence of the shocks on February 7 and March 1, may be related to the fact (usual in such circumstances and here mentioned by several chroniclers) that most people, frightened by the wide-ranging effects of the first two earthquakes, were then camping out of their houses. Such an inference may not hold for the shock on March 28, six weeks after the main February 5 event and nearly 100 km northeast of the Messina strait, hence the relatively large number of fatalities in Borgia (Table 1), which are attributable to that shock only.

Table 1. List of towns and villages where 1783 earthquakes killed more than 300 people, in order of decreasing number of casualties, from Baratta's (1901) table (pp. 284–288).

Locality	Casualties	Locality	Casualties
Bagnara	3331	Radicena	756
Polistena	2261	Messina	617
Casalnuovo (Cittanova)	2017	Molochio	600
Terranova	1458	Varapodio	497
Scilla	1450	Sinopoli	382
Seminara	1370	Galatro	341
Cinquefrondi	1343	Borgia	332
San Giorgio Morgeto	1312	Paracorio	325
Oppido	1198	San Procopio	316
Palmi	999	Iatrinoli	312
Sant'Eufemia di Sinopoli	945	Tresilico	310
Santa Cristina d'Aspromonte	760		

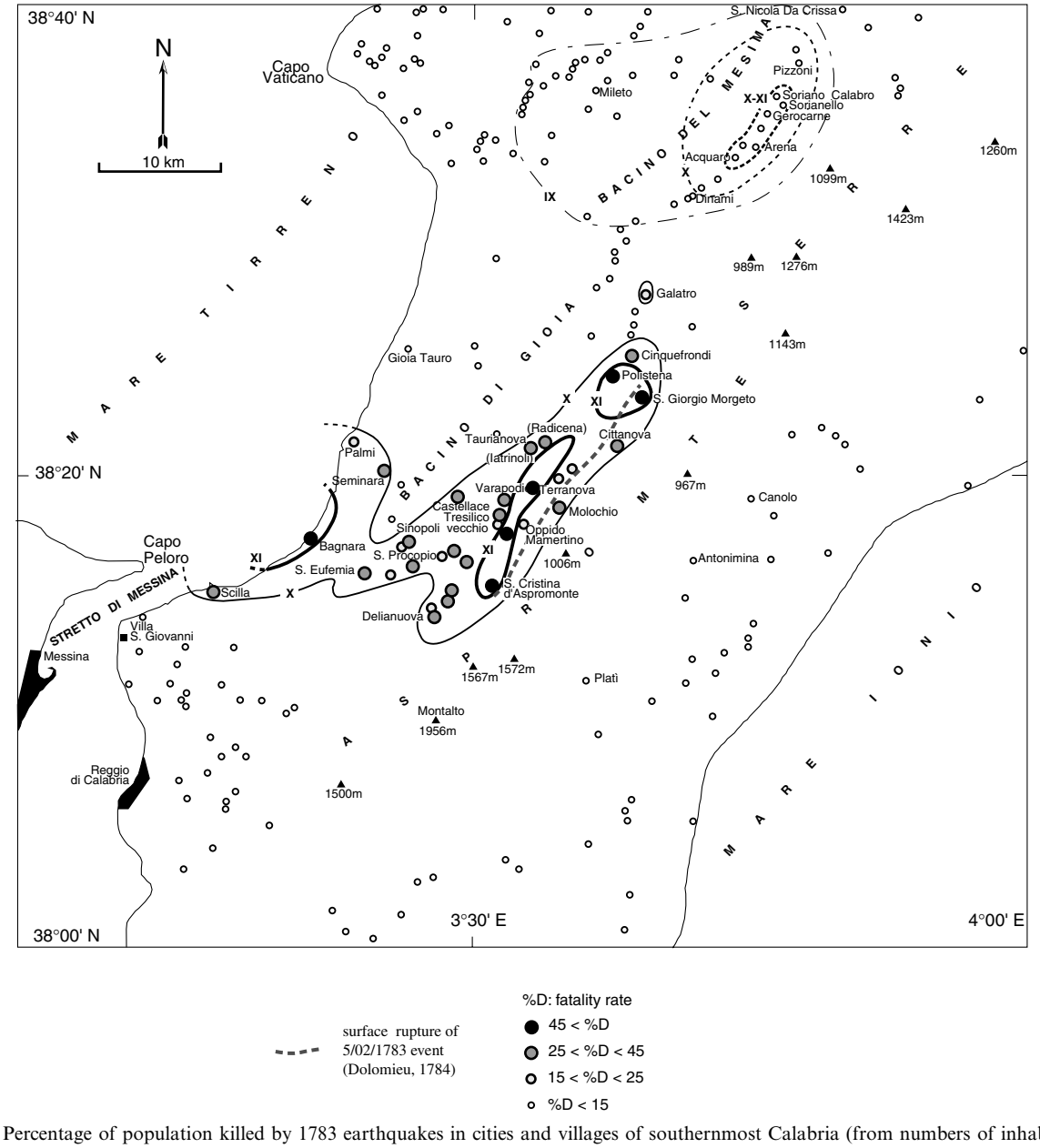

Figure 4. Percentage of population killed by 1783 earthquakes in cities and villages of southernmost Calabria (from numbers of inhabitants and casualties listed by Vivenzio 1783). Solid lines delimit regions with most gravely struck population centres (highest fatality rates, see text for intensity estimates). Fatalities in the area covered by the map, which does not include epicentral areas of the March 1 and 28 shocks (Fig. 3), resulted mostly from shocks on February 5 and 6. Dotted lines represent the isoseismals IX, X and X–XI of the February 7 event according to Boschi *et al.* (1995).

Locations, intensities and inferred magnitudes of the various shocks

The observations compiled in Fig. 4 yield a clear macroseismic picture of the first two shocks of the 1783 sequence. They complement and give firmer basis to inferences made in previous reports (e.g. Baratta 1901) and by those who visited the area at the time. Two features of the zone of maximum ground shaking intensity in Fig. 4 are robust. First, the zone has two main lobes connected by a narrow isthmus near Sant'Eufemia. The smaller lobe roughly coincides with the Palmi high along the Tyrrhenian coast. The larger lobe is a 5–10 km wide, 35 km long strip of the Gioia Basin along the steep northwestern edge of the Aspromonte. Second, shaking intensities seem to have decreased rapidly from peak values causing complete collapse of all constructions and fatality rates of 50 per cent or more along the axial zones of these two lobes to much smaller values, sparing more than 85 per cent of the population less than 10 km away from such paroxysmal zones. These two features imply that the two shocks had distinct hypocentres at shallow crustal depths (<20 km). The most likely locations of the two hypocentres are clearly under the eastern part of the Gioia Basin (probably between Oppido and Molochio) for the main February 5 shock, and off the Tyrrhenian coast (probably between Scilla and Bagnara) for the February 6 shock. Such hypocentres correspond to the sites inferred to have

been the 'centres' of the earthquakes (Fig. 3) at a time when the physical nature of earthquakes was unclear (e.g. Hamilton 1783; Vivenzio 1783; Dolomieu 1784; Baratta 1901; see also Postpischl 1985; Boschi *et al.* 1995). Both earthquakes had pronounced effects on the regional morphology. The first triggered numerous landslides of awesome proportions (referred to as 'sconvolgimento') that dammed rivers to create 215 lakes, five of which were 1 km or more in length (Vivenzio 1783; Cotecchia *et al.* 1969). The second triggered a large, 2 km long rockslide along the Tyrrhenian coastal cliff as well as a small tsunami (Baratta 1901). The first shock also caused the widespread occurrence of sand fountains. It is probable that, as noted by Dolomieu and Baratta, the exceptional size and pervasiveness of such effects was partly a result of the regional geology and of a notably rainy winter. Nevertheless, effects of this type are usually characteristic of intensities of at least X–XI (corresponding to magnitudes ≥ 6.5 using the relationship between magnitude and epicentral intensity I_0 for the Italian peninsula $M = 0.53I_0 + 0.96$; Armijo *et al.* 1986). Hence, it is probably reasonable to infer that the continuous contours drawn in Fig. 4 roughly follow the isoseismals X and XI or XI and XII. The surface area of the zone within the outer contour (intensity X or XI isoseismal) of the largest lobe suggests, in turn, that the magnitude of the first, main February 5 shock was at least equal to 7, as implied by its large environmental effects, corresponding to intensities of XI–XII (see also Postpischl 1985; Boschi *et al.* 1995). Similarly, the second, February 6 shock probably reached an intensity of about X–XI, corresponding to a magnitude of at least 6.5.

Like the first two events, the two subsequent events of the 1783 Calabrian earthquake sequence were probably shallow crustal events. They were smaller than the main February 5 shock. The February 7 earthquake was clearly larger than the March 1 shock. As implied by the contours of the mesoseismic area (Fig. 3), the February 7 event was located in the southeastern part of the Mesima Basin, at the western foot of the Serre Mountains, where it reduced to heaps of ruins all the villages between Acquaro and Soriano Calabro, and caused destruction between Pizzoni and Dinami (a distance of 15 km; Fig. 4), with landslides in the vicinity of Soriano, Arena and Mileto (e.g. Dolomieu 1784; see also Boschi *et al.* 1995). Note that since most of the inhabitants were camping out of their houses at this time, the percentage of casualties cannot be used to assess the size of the earthquake. The March 1 event was located along the northernmost edge of the Mesima Basin, at the northwestern foot of the Serre Mountains, where it caused more limited damage (Fig. 3, see also Postpischl 1985; Boschi *et al.* 1995). Thus, while the February 7 shock could have reached an intensity of X or slightly more (Fig. 4, see also Boschi *et al.* 1995) and a magnitude of at most 6.5, that on March 1 probably had an intensity of IX at most (e.g. Postpischl 1985) and a magnitude smaller than 6. For the March 28 event, the mesoseismal area (Fig. 3) suggests a location in the Catanzaro Basin, near Borgia, about 20 km WNW of the March 1 event. It may have reached an intensity of XI (according to Boschi *et al.* 1995) and a magnitude of the order of, or somewhat greater than, 6.5. However, this shock appears to have been deeper than the previous ones. The gradient defined by the isoseismals, which is less steep than that associated with the main event of February 5 (Fig. 3), and the fact it was felt at greater distances (Baratta 1901) attest to a deeper rupture nucleation.

RECENT AND ACTIVE FAULTS OF SOUTHERN CALABRIA

The main normal fault system separating the South Calabrian Upper Pliocene–Pleistocene basins from the uplifted mountain ranges comprises chiefly, from north to south, the Serre Fault, along the west side of the Serre Mountains, the Galatro, Cittanova (Santa Cristina) and Sant'Eufemia faults, along the northwest edge of the Aspromonte massif, and the Scilla Fault, bounding the Palmi high along the Tyrrhenian Sea (Figs 1 and 2).

Given the Plio-Quaternary geological framework, the inference drawn from the macroseismic observations that the 1783 February 5 and 6 earthquakes had their hypocentres at shallow depths just west of the Aspromonte and Palmi highs (Figs 1 and 3) implies that these two earthquakes resulted from slip on the west-dipping normal faults bounding these two basement highs. Similarly, the February 7 and March 1 earthquakes resulted from slip on the west-dipping normal fault separating the Serre basement high from the Mesima Basin.

Morphological and structural evidence confirms these conclusions and yields first-order constraints on the kinematics and rates of active faulting in this southernmost part of Calabria.

Surface break of the 1783 February 5 earthquake on the Cittanova Fault

Alone among the scholars and engineers who visited southern Calabria after the 1783 earthquakes, Deodat Gratet de Dolomieu was a dedicated Earth Scientist. His description of the mesoseismal area of the Calabrian earthquakes (Dolomieu 1784) places the morphological effects of these earthquakes in a geological framework that is clear and correct by modern standards. Although Dolomieu did not understand the origin of the earthquakes at the time, his accurate observations throw definitive light on surface deformation. Two paragraphs of his 'Mémoire' (Dolomieu 1784, p. 36 and p. 46), which we quote fully below, provide the key:

'Il s'ensuivit, que dans presque toute la longueur de la chaine, les terreins, qui étoient appuyés contre le granit de la base des monts Caulone, Esope, Sagra et Aspramonte, glissèrent sur ce noyeau solide, dont la pente est rapide, et descendirent un peu plus bas. Il s'établit alors une fente de plusieurs pieds de large, sur une longueur de 9 à 10 milles, entre le solide et le terrein sabloneux; et cette fente règne, presque sans discontinuité, depuis Saint George, en suivant le contour des bases, jusque derrière Sainte Cristine.'

'Tout le sol de la plaine, qui entoure Casalnovo, s'est affaissé. Cet abaissement est surtout fort aparent, au dessus du bourg, au pied de la montagne. Tous les terreins inclinés, apuyés contre cette même montagne, ont glissé plus bas; en laissant, entre le terrein mouvant et le solide, des fentes de plusieurs pieds de large, qui s'étendent à trois, ou quatre milles.'

['Along almost the entire length of the range, the rocks that were standing against the granite at the base of Mts Caulone, Esope, Sagra and Aspramonte slipped on that rigid core, whose slope is steep, and descended a little lower. Thus was established a fissure several feet wide, over a length of 9–10 miles between the solid rock and the sandy terrane, and this fissure prevails, almost without discontinuity, from San Giorgio, following the contour of the mountain base, as far as behind Santa Christina.'

'The floor of the whole plain around Casalnuovo fell down. Such downthrow is mostly apparent above the village, at the foot of the mountain. All the sloping terranes that stood against this mountain slid down, leaving, between the solid rock and the moving terrane, open fissures several feet wide over a length of 3–4 miles.']

The length, continuity and position of the zone of downthrow and fissures, along the interface between bedrock and Quaternary sediments, leave little doubt that Dolomieu, while interpreting this zone as the trace of an exceptionally large landslide, linked to regional compaction, was in fact the first to describe the surface break of an earthquake.

From Dolomieu's observations, it was clearly the Cittanova Fault that ruptured over a length of 18 km during the 1783 February 5 main shock. Seismic slip on the fault appears to have been the largest between S. Giorgio and S. Cristina, possibly with a maximum near Molochio. The presence of open fissures at the base of the coseismic scarp is in keeping with extensional faulting, with slip on the fault plane at depth propagating more steeply near the surface, giving rise to cracks, as commonly observed, for instance, in Afar (Jacques 1995). The reported crack opening (several feet) was probably of the order of 3–4 ft (>2), corresponding to a width $=1$ m (the foot size used by Dolomieu was equal to ~ 0.32 m). On a fault plane dipping $\sim 70^\circ$ near the surface, such a width would be consistent with about 3 m slip. This motion clearly occurred along the forested slope break still visible above the olive groves at the range-front base near Molochio (Fig. 5a).

Geomorphological and structural evidence for active faulting along the northwestern edge of the Aspromonte and Serre mountains

There is much structural and geomorphological evidence confirming recent, ongoing movement on the normal faults of southern Calabria. The faults clearly cut and deform the Upper Pleistocene beach sands deposits (Tortorici *et al.* 1995) and control the regional topography (Figs 5 and 6) giving rise to prominent range-front escarpments (Tapponnier *et al.* 1987), along which other large earthquakes have destroyed towns and villages in the past (e.g. 1659 and 1791, Fig. 1).

The 40 km long cumulative escarpment of the NNE–SSW-trending, WNW-dipping Serre Fault is up to 200 m high (Fig. 7a). The footwall basement rocks are overlain by two terrace levels of Early Middle Pleistocene age (Ghisetti 1981). Narrow V-shaped valleys separate well-developed triangular or trapezoidal facets along the range front. The NNE-trending Galatro Fault, within the left step between the Serre and Cittanova faults, is only 6 km long, with a 150 m high cumulative escarpment (Figs 1 and 7b). This short fault is probably the northernmost segment of the ~ 40 km long, NE-trending Cittanova Fault, with which it may merge at depth.

Along the Cittanova Fault, the Upper Pleistocene sands are strongly tilted westwards and cut by numerous secondary faults, some of them rotated into reverse attitude (Fig. 5b). A 1–2 m wide gouge zone separates the sands from the crystalline basement rocks. Mesostructural analysis of the gouge indicates dip-slip movement and N140°E $\pm 10^\circ$ extension (Tapponnier *et al.* 1987; Tortorici *et al.* 1995). The morphology of the Cittanova Fault escarpment varies along strike. The 10 km long southwestern stretch of the fault is marked by a cumulative scarp of rather small height (100–150 m), while towards the northeast this scarp (~ 30 km long) reaches a height of 400–700 m (Figs 5a, 6 and 7c). This highest part of the escarpment is shaped by three sets of triangular facets (Tortorici *et al.* 1995). It is at the base of the lowest facets that Dolomieu described the most prominent break of the main shock of the 1783 sequence (Tapponnier *et al.* 1987), suggesting a relationship between largest slip per event, fastest slip rate and greatest finite offset. While the footwall to the southwest is overlain by only one Lower Pleistocene terrace (Fig. 2), a second terrace level of Mid-Pleistocene age (Ghisetti 1981; Dumas *et al.* 1982) exists in the northeast (Figs 2a, 5a and 7c). Because Pleistocene marine sedimentation reached the range front in the northeast, it is likely that the different sets of facets and terrace levels there correlate with climatic sea-level highstands. Stratigraphic and geomorphological data suggest a minimum vertical slip rate along the Cittanova Fault of 0.7 mm yr^{-1} in the last 125 kyr (Tortorici *et al.* 1995). We interpret the smaller vertical throw on the southwestern stretch of the Cittanova Fault as resulting from a combination of strike change and slip transfer. The more westerly strike of this stretch implies a sinistral component of slip, as observed in the field (Tortorici *et al.* 1995) (Fig. 1, inset). More importantly, extension is probably distributed between this stretch and the nearby Sant'Eufemia Fault, as commonly observed along overlapping normal fault systems (e.g. Manighetti *et al.* 2001a,b).

West of the Delianuova right step, the 18 km long, ENE–WSW-trending Sant'Eufemia Fault dips to the NNW, bounding the southern sector of the Gioia Tauro Basin (Figs 1, 2 and 6). The cumulative escarpment of this fault is up to 300 m high (Fig. 7d). Its southwestern part, ~ 10 km long, displays two sets of triangular facets separated by wine-glass valleys (see Fig. 7 in Tortorici *et al.* 1995), with two distinct terrace levels of Lower–Middle Pleistocene age on the uplifted footwall (Ghisetti 1981; Dumas *et al.* 1982). Shear planes in crystalline footwall rocks show oblique slickensides (pitches of 35°–70°) consistent with a left-lateral component of slip and a N135°E $\pm 5^\circ$ extension direction (Fig. 1, inset) (Tortorici *et al.* 1995). An uplift rate of ~ 0.7 mm yr^{-1} in the last 125 kyr, comparable to that on the Cittanova Fault, has been estimated on this fault (Tortorici *et al.* 1995).

Finally, the NW-dipping, NNE–SSW-trending Scilla Fault bounds the Tyrrhenian shore of the Palmi high (Figs 1 and 2). Southwest of Bagnara it veers to an ENE–WSW direction, which it keeps onland to Villa San Giovanni. Between Bagnara and Scilla, the escarpment forms a sea cliff up to 600 m high (Fig. 7e). The crystalline rocks of the footwall are capped by a Middle Pleistocene marine terrace, tilted towards the southeast (Ghisetti 1981; Dumas *et al.* 1982). Southwest of Bagnara, up to four levels of uplifted marine terraces (Figs 2 and 7e), reflecting Middle–Upper Pleistocene sea-level highstands (Valensise & Pantosti 1992; Westaway 1993; Tortorici *et al.* 1995), appear to correspond to isotopic stages 11, 9, 7 and 5 (Bassinot *et al.* 1994). East of Villa San Giovanni, the 90 m offset of the lower level (stage 5) is again consistent with a throw rate of about 0.7 mm yr^{-1} in the last 125 kyr.

MODELLING OF STATIC STRESS CHANGES INDUCED BY THE 1783 SEISMIC SEQUENCE

Following the overall approach taken by Reasenberg & Simpson (1992) and King *et al.* (1994), we model the faults as

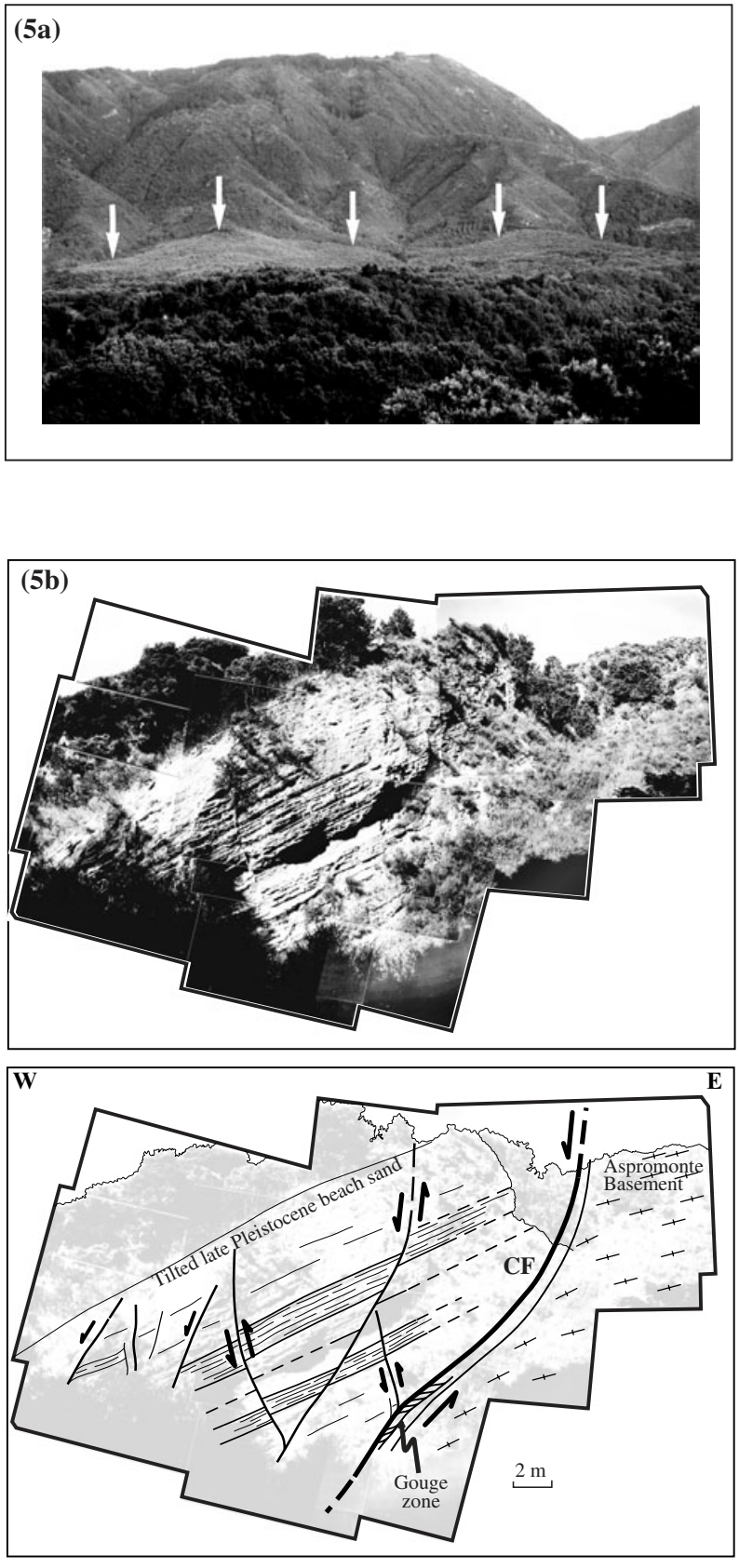

Figure 5. (a) Aspromonte front near Molochio (shown in Fig. 2 by a dotted box). Slope break at base of faceted spurs (arrows) corresponds to trace of Cittanova (Santa Cristina) Fault and to part of the 1783 surface scarp mentioned by Dolomieu (1784). (b) Cittanova Fault zone (site indicated by an arrow in Fig. 2). Normal masterfault (CF) separates footwall Aspromonte gneisses to the southeast (right-hand side of photomontage) from upper Pleistocene Gioia Basin beach deposits in hangingwall (left-hand side). View to NE. Pleistocene deposits are strongly tilted ($\approx$ N40°E, 35–40°NW) and faulted. Several faults striking parallel to CF (N40°E) have steep eastward dips and appear to be normal faults tilted into reverse position.

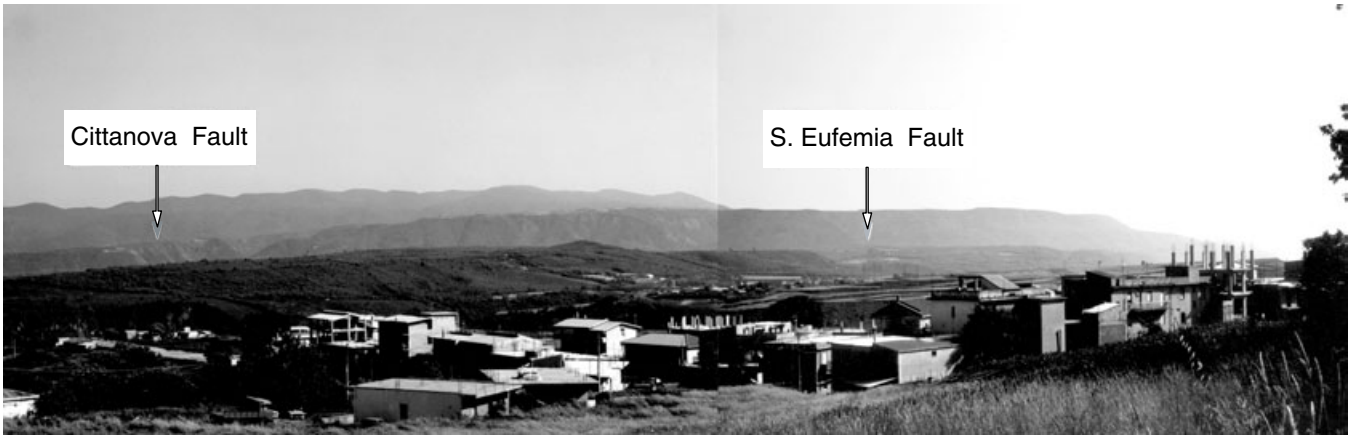

Figure 6. General view of uplifted basement steps along the Sant'Eufemia and Cittanova (Santa Cristina) faults (looking SSE from Sant'Elia Mountain near Palmi), triangular dotted line box in Fig. 2. Gioia Tauro Basin is in the foreground.

discontinuities in an elastic half-space. To study the effect of stress changes caused by the successive ruptures of different fault segments during the earthquake sequence, we calculate the changes of the Coulomb failure stress σ_f on either optimally oriented fault planes or fault planes with given strikes ($\Delta\sigma_f = \Delta\tau - \mu'\Delta\sigma_n$, where $\Delta\sigma_n$ and $\Delta\tau$ are changes in normal and shear stresses on the fault planes and μ' is the effective friction coefficient). Following King *et al.* (1994), optimum fault angles are determined using the stress field obtained by adding a regional stress field to that created by the seismic dislocations and calculating the directions that maximize σ_f on those planes. The areas where σ_f increases are those where subsequent brittle failure is promoted. Where σ_f drops, faulting is less probable.

Parameters used for Coulomb modelling

From focal depth determinations of the 1908 and 1975 Messina Strait earthquakes (Gasparini *et al.* 1982; Cello *et al.* 1982; Bottari *et al.* 1989), we infer the regional seismogenic thickness to be $\sim$20 km. This is compatible with the maximum magnitude ($\sim$7) of known crustal events. We thus take the maximum depth of seismic faulting to be 20 km. We show the results of Coulomb stress calculations at a depth of 10 km (mid-depth of the seismogenic crust), using a standard shear modulus of 3.3×10^{10} Pa and a friction coefficient of 0.75. Given the size of the first three events, which implies a $\sim$15 km depth of nucleation, the 10 km depth choice seems adequate. For the probably shallower 1783 March 1 $M \sim 5.7$ event ($\sim$6 km), a depth of 5 km was chosen to assess the triggering effects of previous shocks. In any case, $\Delta\sigma_f$ is not very sensitive to depth, except close to faults, where small uncertainties in parameters such as dip, strike, slip distribution, fault length and sinuosity can lead to significant changes. Similarly, the choice of the modulus only changes the absolute values of σ_f. Errors in estimating the seismic moment only change σ_f amplitudes. The value of the friction coefficient, which is also not very critical (King *et al.* 1994), is selected to be consistent with observations, as discussed below.

In southwestern Calabria, the recent extension direction inferred from slickenside measurements is about N125°E (Cello *et al.* 1982; Tortorici *et al.* 1995), compatible with the fault plane solutions of five out of seven shallow events (December 1908, January 1975, April 1978 and February 1980) (Cello *et al.* 1982; Gasparini *et al.* 1982; Anderson & Jackson 1987). Three solutions show dominant dip slip on N10°E–N50°E-striking normal faults. The other two are dominantly strike-slip on either N30°E–N60°E-striking left-lateral planes or N120°E–N150°E-striking right-lateral planes. Leaving aside the 1947 and 1990 events, located on the outer fringe of the region of interest, we thus take a N125°E regional extension direction for modelling. In general, regional stress magnitudes are poorly known. We use a low value (40 bar) for the regional deviatoric extensional stress σ_3. The results would not be significantly altered by choosing a higher value. Moreover, as pointed out for strike-slip faulting by King *et al.* (1994), the $\Delta\sigma_f$ distribution is relatively insensitive to the amplitude of the regional stress.

Except very close to the faults, the friction coefficient and stress direction chosen yield optimum left-lateral faults orientated N70°E and normal faults striking N35°E. This is compatible with the observed direction of left-lateral (N45°E–N90°E) and normal faults (N25°E–N45°E) in the field (Tortorici *et al.* 1995). The relatively high value of the friction coefficient (0.75) chosen yields an optimum dip of $\sim$63° for the optimal normal fault, consistent with the dips observed in the cross-sections [Figs 1 (inset), 2 and 6] (Tortorici *et al.* 1995).

Seismic slip during the 1783 February 5 event

The location of the main 1783 February 5 shock (Fig. 3) and the corresponding fatality distribution (Fig. 4) imply that it resulted from rupture of three fault segments (Cittanova, Sant'Eufemia and Galatro). Given the length of surface rupture and maximum slip observed by Dolomieu, it is likely that the entire northeasternmost 30 km of the Cittanova Fault, near which the most extensive destruction occurred, slipped during the main shock. The Sant'Eufemia Fault, along which damage and casualties were similarly great on February 5, probably slipped at about the same time over a minimum length of $\sim$10 km. The 6 km long Galatro Fault, which extends beyond the NE end of the Cittanova Fault did not generate a separate event, but probably also slipped at the time of the main shock. This interpretation brings the total length of faulting during the February 5 event to $\sim$45 km. With a mean fault dip of $\sim$65°, the overall rupture area is about 1000 km^2. The empirical magnitude versus rupture area relationship of Wells & Coppersmith

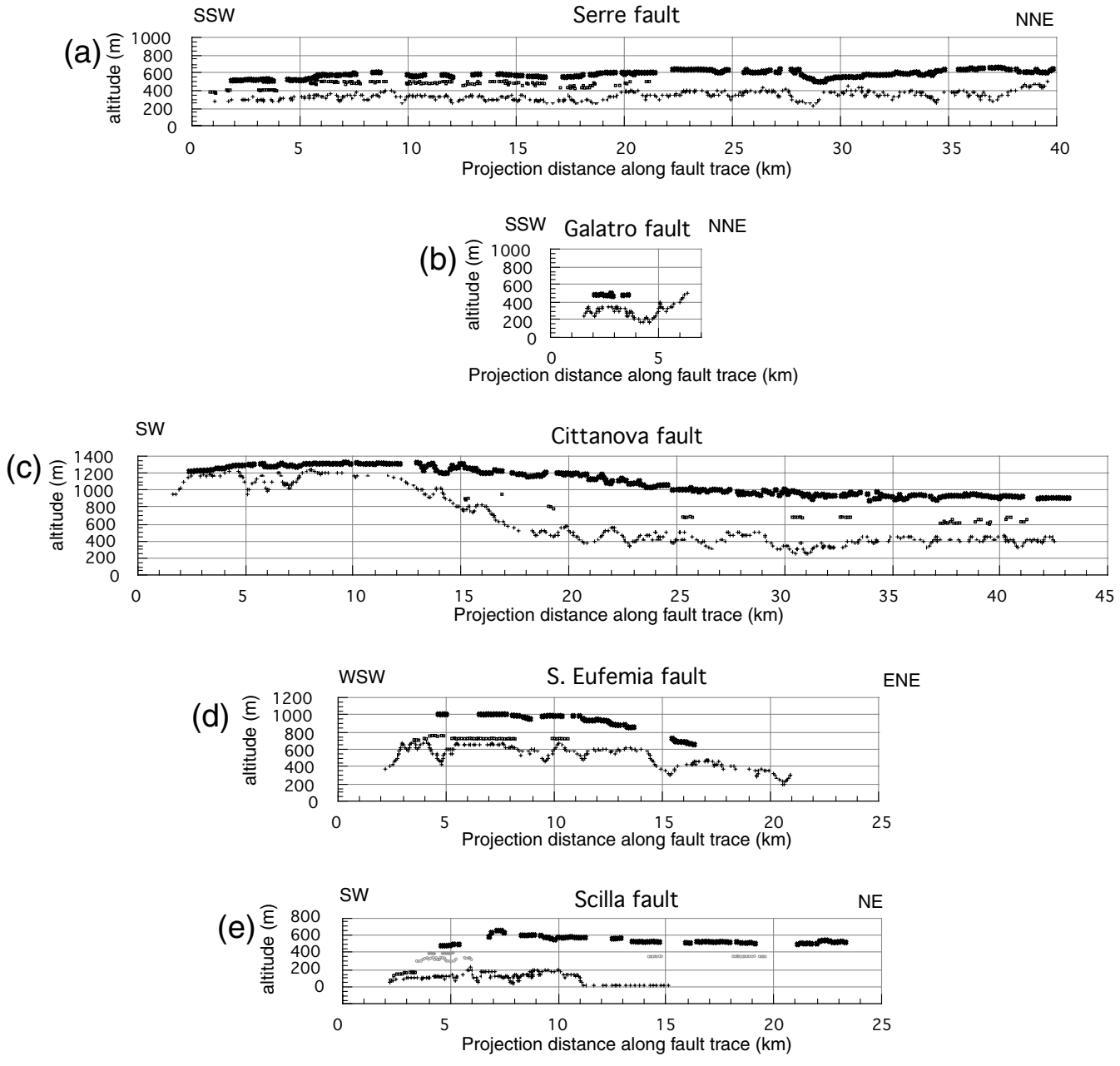

Figure 7. Projections, on appropriately oriented vertical planes, of topographic profiles along (a) the Serre (N30°E), (b) the Galatro (N20°E), (c) the Cittanova (N40°E), (d) the Sant'Eufemia (N70°E) and (e) the Scilla (N45°E) fault traces (crosses), and along the outer edges of terrace levels (open squares, grey dots and black diamonds) preserved on footwalls (from IGM 1:25 000 topographic maps). Vertical exaggeration is 4. Minimum cumulative vertical offset is between the upper terrace level (black diamonds) and the fault trace (crosses).

(1994) would thus imply a magnitude of ~ 7 for this shock. Other scaling laws (Scholz 1990; Jacques 1995) would yield a magnitude of about 7.2, or a seismic moment, M_0, of $\sim 7 \times 10^{19}$ Nm. All these estimates are in agreement with the magnitude inferred from discussion of the mesoseismal macroseismic effects. Finally, an M_w magnitude of ~ 7.2 would imply an average slip of ~ 2 m using the magnitude relationship $M_w = (2/3)\log(\mu S \Delta u) - 6.03$ of Kanamori (1977). This is also consistent with the maximum slip of ~ 3 m observed on the Cittanova Fault by Dolomieu (1784), and with the empirical relationship between maximum slip and magnitude of Wells & Coppersmith (1994).

Instead of using the same average slip value on the three fault segments ruptured by the February 5 main shock, one may use long-term geomorphological evidence to estimate the relative amplitudes of average seismic slip on the Galatro, Sant'Eufemia and Cittanova faults. We assume the average seismic slip (Δu) to be linearly related to the apparent cumulative vertical offset (Cvo) on each fault (King *et al.* 1988) ($\Delta u = a\mathrm{Cvo} + b$). a and b can be derived from the values observed along the Cittanova Fault ($\Delta u \sim 2.5$ m, between the average of 2 m and the maximum value of 3 m; Cvo = 440 m) and from the condition that the total moment resulting from coseismic slip on the three faults is $\sim 7 \times 10^{19}$ N m (Table 2). We obtain $a = 0.0054$ and $b = 0.0436$ m. We also assume a uniform orientation of the slip vector on the three faults, which yields dip values of 60°, 65° and 70° for the Cittanova, Galatro and Sant'Eufemia faults,

Table 2. Fault parameters used in Coulomb modelling.

Fault segment:	Galatro	Cittanova	Sant'Eufemia
Mean apparent cumulative vertical offset (m)	150	450	300
Mean dip (°)	65	60	70
Surface of broken segment (km^2)	134	655	219
Seismic slip (m)	0.9	2.5	1.7
Pitch	95°N	90°	75°W

respectively (Table 2). Given the mean strike of the Cittanova Fault (N40°E), which is nearly orthogonal to the regional extension direction (N125°E), consistent with pure normal faulting, this kinematic compatibility condition also yields pitches of 95°N and 75°W on the Galatro and Sant'Eufemia faults, respectively, in agreement with field observations (Fig. 1, inset) (Tortorici *et al.* 1995). The final parameters used as inputs for the Coulomb modelling on each fault segment are given in Table 2.

Coulomb stress changes caused by the 1783 February 5 main shock on the fault of the 1783 February 6 event

The main shock increased σ_f by more than 10 bar both north of Galatro and west of Sant'Eufemia, whether on normal faults striking N35°E and N70°E (Fig. 8a) or on optimally oriented strike-slip faults (left-lateral, striking ~N70°E, Fig. 8b).

Thus, the February 5 earthquake most probably promoted rupturing of the N70°E-trending, southwest part of the Scilla Fault. Considering only static stress changes, the rupture might have stopped near Bagnara (where the fault bends to a NNE direction), but macroseismic observations (Fig. 4) suggest that it propagated northeastwards to Palmi.

Seismic slip during the 1783 February 6 event

According to models of circular rupture (e.g. Scholz 1990) and assuming a stress drop of 30 bar (an average value, Kanamori 1977), the rupture diameters of $M=6$–6.5 earthquakes range between 11 and 19 km. With a mean dip of about 65°, such ruptures would cut the crust to depths of 10–17 km, falling short of the base of the seismogenic layer, in keeping with the use of such models.

The length of the Scilla Fault lying within the area of high σ_f increase is about 14 km, suggesting a minimum equivalent circular rupture surface of 16 km diameter. This corresponds to a minimum seismic moment of $\sim 3.7 \times 10^{18}$ Nm (average minimum $\Delta u = 0.55$ m) and a minimum magnitude M_w of ~6.3. This lower bound is compatible with the magnitude (≥ 6.5) derived from macroseismic observations, which suggest that the rupture propagated to Palmi over a total length of ~20 km. To examine the effects of static stress change, we use a square rupture with a side length of 14 km, keeping in mind that such effects are minimized by this choice.

Because the macroseismic effects of the February 6 shock include a tidal wave, we assume that the rupture reached the surface. We take the fault dip to be ~65° and the pitch or rake of the slip vector to be identical to that on the Sant'Eufemia Fault, almost parallel to the trace of the southwest part of the Scilla Fault.

Coulomb stress changes caused by the February 5 and 6 events on the fault of the 1783 February 7 event and in the Messina Strait

After the February 5 and 6 shocks, σ_f rose by more than 1–5 bar on the southwest part of the Serre Fault where the February 7 event took place (Fig. 8c). This fault is nearly parallel to optimally oriented normal faults, suggesting that the combined effects of the first two events promoted the occurrence of the February 7 shock.

Another, smaller event occurred in the evening of February 7 (22:00 local time), about 2 hr after the third principal shock of the sequence, and was destructive mostly at Messina and to a lesser degree at Sant'Agata di Reggio. This earthquake was probably located in the Messina Strait region (Baratta 1901) within the area where the Coulomb stress rose by 1–5 bar south of the Scilla and Sant'Eufemia faults (Figs 1, 8c and 8d).

Seismic slip during the 1783 February 7 and 1783 March 1 events

The macroseismic effects of the February 7 event are consistent with a magnitude of ~6.5 and a seismic moment of $\sim 6.2 \times 10^{18}$ Nm. Using the circular rupture model and the same assumption on stress drop as for the February 6 event, we approximate the source by a square-shaped rupture with a side length of 17 km centred on the area of maximum destruction. As for the February 6 shock we assume a fault dip of 65°, and that the rupture nearly reached the surface. The segment of the Serre Fault activated by the February 7 earthquake (average $\Delta u = 0.65$ m) lies fully within the area where σ_f increased between 1 and 10 bar due to the previous 1783 events (Fig. 8c). However, between the Galatro Fault, which we infer to have slipped during the main shock, and the 17 km long segment of the Serre Fault broken by the February 7 event, there still exists a 4 km long stretch of the Serre Fault that seems not to have ruptured (Figs 1 and 8d) although it lies in an area where σ_f rose by 5–10 bar. Other than an unreported fore- or aftershock, or aseismic strain relaxation, one possible explanation for this apparent rupture gap is that we have underestimated the rupture length of the February 7 event.

The 1783 March 1 event appears to have also ruptured the Serre Fault further north, but its macroseismic effects imply a magnitude of only ~5.7 and a seismic moment of $\sim 3.9 \times 10^{17}$ Nm. Using the same assumptions as for the February 6 and 7 events, its source parameters (including an average $\Delta u = 0.30$ m) may be approximated by a shallow square-shaped rupture surface with a side length of ~7 km centred on the area of maximum destruction with a dip of 65° and reaching a depth of ~6 km below the surface.

Coulomb stress changes caused by previous 1783 events on the fault of the March 1 event

Fig. 8(d) shows the $\Delta\sigma_f$ caused by the first three shocks of the 1783 sequence computed in this case on optimally oriented normal faults at a depth of 5 km, near the bottom of the inferred source of the March 1 event, consistent with the usual nucleation depth of $M > 5$ earthquakes. That the fault segment that activated the March 1 earthquake is oriented nearly parallel to the optimal normal faults and lies in an area where σ_f

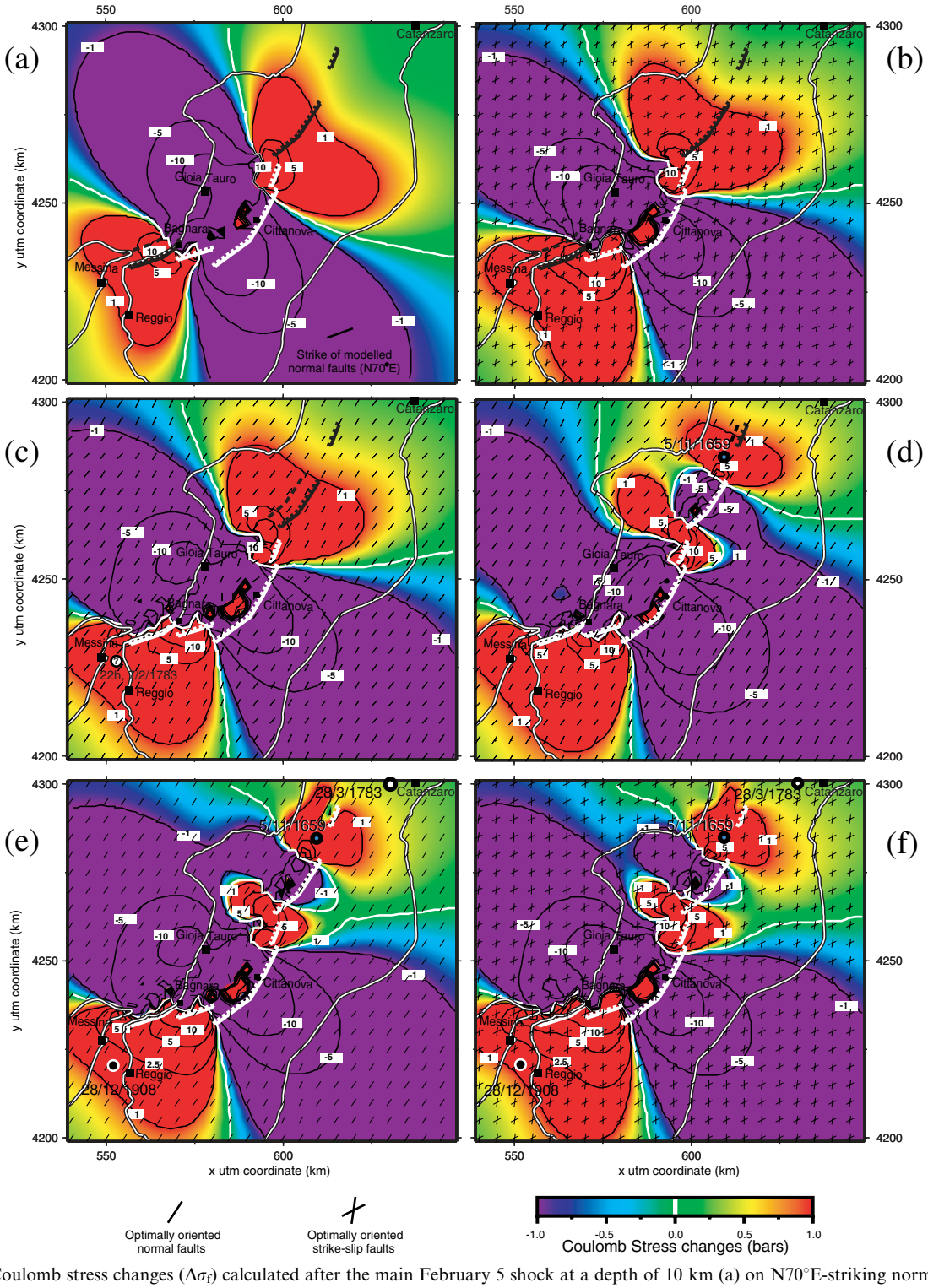

Figures 8. Coulomb stress changes ($\Delta\sigma_f$) calculated after the main February 5 shock at a depth of 10 km (a) on N70°E-striking normal faults and (b) on optimally oriented strike-slip faults (regional $\sigma_3 \sim$ N125°E). Ruptured fault segments are drawn in white. The trace, at 10 km depth, of the Scilla Fault is drawn as a black dashed line. From (a) it appears that failure on the Scilla Fault is promoted, and from (b) a component of sinistral strike-slip is expected. (c) Coulomb stress changes ($\Delta\sigma_f$) calculated after the February 5 and 6 earthquakes on optimally oriented normal faults (ruptured fault segments are drawn in white). The trace of the southern part of the Serre Fault, at 10 km depth, is drawn as a black dashed line. It appears that failure on the southern part of the Serre Fault (1783 February 7 event) is promoted (Coulomb stress increase from 1 to 5 bar). (d) Coulomb stress changes ($\Delta\sigma_f$) calculated at 5 km depth after the February 5, 6 and 7 earthquakes on optimally oriented normal faults (ruptured faults segments drawn in white). The trace of the northern part of the Serre Fault, at 5 km depth, is drawn as a black dashed line. It appears that the Coulomb stress increased by about 1 bar on the northern part of the Serre Fault (1783 March 1 shock). The 1659 November 5 event is plotted on this figure as a black-circled blue dot. Coulomb stress changes ($\Delta\sigma_f$) calculated after the February 5, 6, 7 and March 1 earthquakes (e) on optimally oriented normal faults and (f) on optimally oriented strike-slip faults at 10 km depth. The 1783 March 28 event is plotted on these figures as a black-circled white dot. Note that the 1908 December 28 earthquake (white-circled black dot) located in the Messina Strait lies in a area where σ_f increased by about 2 bar on SSE-striking normal faults. The 1659 November 5 event is plotted on these figures as a black-circled blue dot; it could have previously ruptured the central segment of the Serre Fault.

rose by ~1 bar after the February 7 event is consistent with the idea that this event was triggered by the first three events of the 1783 sequence.

Effects of Coulomb stress changes caused by the first four shocks of the 1783 Calabria sequence and by the 1659 and 1693 events on subsequent earthquakes

Although within a zone of strong σ_f increase (1–5 bar) following the February 7 event, the central portion of the Serre Fault apparently remained a rupture gap in 1783. We suggest that this is because that stretch of the fault had already ruptured 124 yr previously. Reports of damage and casualties, which were extensive and serious (Baratta 1901), show that the 1659 November 5 earthquake (I_0 = X, Boschi *et al.* 1995; corresponding to $M \sim 6$) (Figs 1, 8e and 8f) was probably due to slip on the central Serre Fault. This event probably ruptured the middle 10 km long segment of the fault, causing on it a decrease of σ_f that remained large enough, over a century later, to prevent rupture.

Figs 8(e) and (f) show the $\Delta\sigma_f$ caused by the first four earthquakes of the 1783 sequence, at 10 km depth, on optimally oriented normal or strike-slip faults. The largest increases, with $\Delta\sigma_f$ reaching more than 10 bar, occur south of the Scilla and Sant'Eufemia faults and in the central overstep between the Cittanova, Galatro and Serre faults. Along the northern part of the Serre Fault, the σ_f increase is only slightly over 5 bar.

Including the $M \sim 6$ 1659 earthquake in the Coulomb modelling, with assumptions similar to those used for the 1783 February 7 shock, augments the σ_f increase in the region immediately west of the epicentre of the 1783 March 28 shock, the last of the sequence, near Borgia, south of the Catanzaro Basin (Figs 1 and 9). Assuming that this event nucleated in the upper crust on an optimally oriented normal or strike-slip fault, the σ_f increase would be only ~0.3 bar without the 1659 event (Figs 8e and f) and between 0.6 and 1 bar with it (Fig. 9). This could account for the triggering of the last event, possibly along a left-lateral strike-slip fault orientated WSW–ENE, in keeping with the maximum elongation of the mesoseismal area (Fig. 3).

The trace and nature of the fault that slipped during this last event remain unclear, however, and the hypocentre depth uncertain, although probably deeper than that of the others. If, as has been inferred from macroseismic evidence reported by Boschi *et al.* (1995), the 1783 March 28 shock had a magnitude of ~6.8 and a seismic moment of $\sim 1.8 \times 10^{19}$ N m, the circular rupture model would yield a dislocation area 28 km across, implying that this event, if shallow, should have cut through the seismogenic crust, causing clear surface breaks. The lack of evidence for coseismic surface faulting is thus in keeping with deeper nucleation. All this prevents us from drawing firmer conclusions about the triggering of this event, and from introducing it in further Coulomb modelling.

One last, minor shock of the sequence, followed by an aftershock swarm, occurred on April 26 1783 (Baratta 1901)

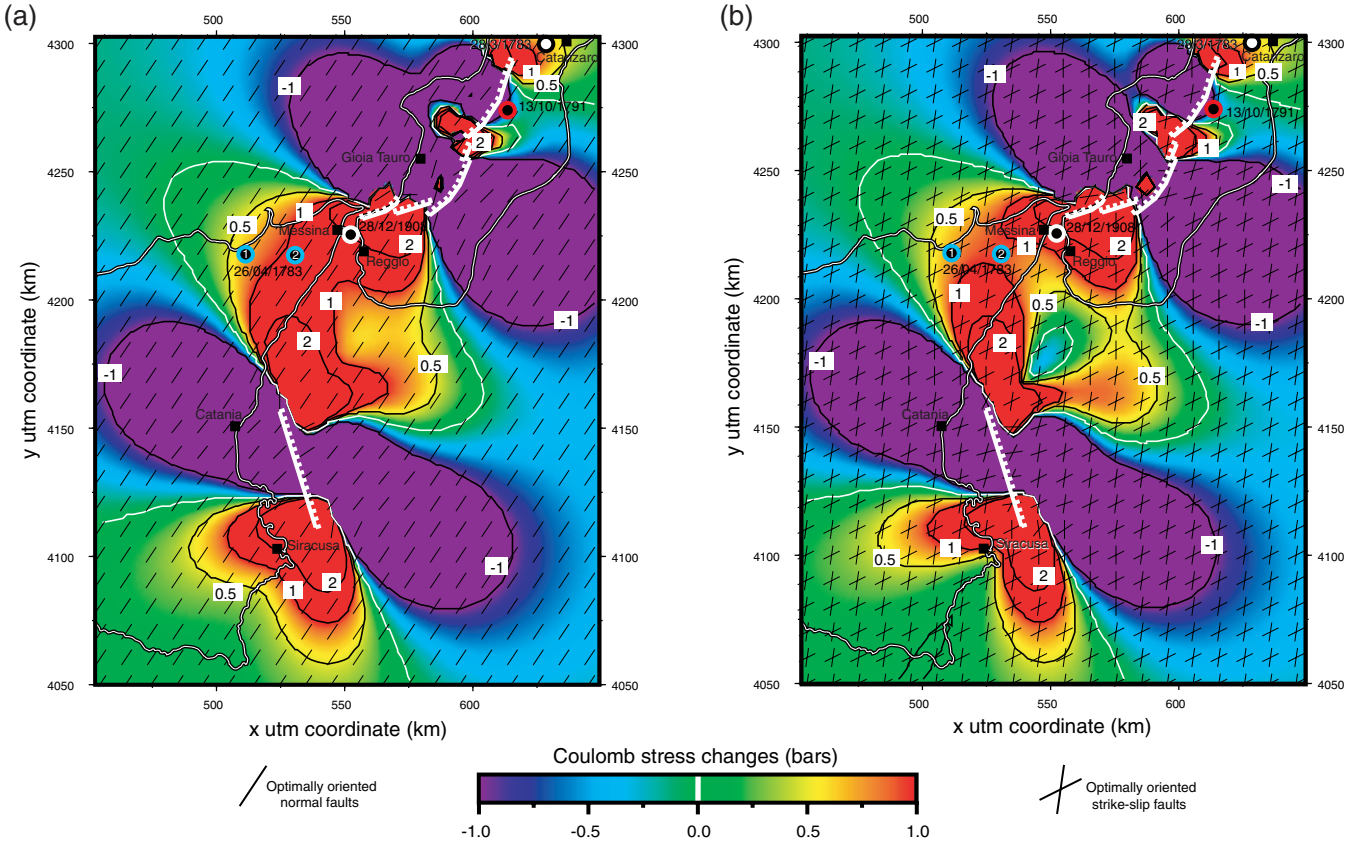

Figure 9. Coulomb stress changes ($\Delta\sigma_f$) calculated after the November 1659, January 1693, February 5, 6, 7 and March 1 earthquakes (a) on optimally oriented normal faults and (b) on optimally oriented strike-slip faults at 10 km depth. The 1783 March 28 Catanzaro Basin earthquake (black-circled white dots), the two locations of the 1783 April 26 NE Sicily earthquake (blue-circled black dots), the 1791 October 13 Serre Mountain earthquake (red-circled black dots) and the 1908 December 28 Messina Strait earthquake (white-circled black dots) are plotted.

($I_0 \sim$ VI–VII, Boschi *et al.* 1995; probably corresponding to $M \sim 4.5$). Although poorly located, it shook the region west of Messina, probably where the σ_f increase following the entire sequence was greater than ~ 1 bar (Figs 8e and f). Although Holocene normal fault scarps have been mapped in the Peloritan Mountains west of the Sicilian coast and north of Etna (Mount Kalfa Faults, Hippolyte & Bouillin 1999), the evidence at hand is insufficient to link the April 26 event with faults in that area.

Of the three moderate to large earthquakes that struck southern Calabria and eastern Sicily in the following 125 yr, two are difficult to reconcile with stress changes induced by the 1783 normal faulting sequence. The 1791 October 13 earthquake (intensity IX) again shook the mesoseismal zone of the 1783 February 7 and 1659 November 5 events (Fig. 1) with an epicentre either in the Serre Mountains between Soriano and Spadola (Boschi *et al.* 1995) or along the coast (Postpischl 1985), northwest of the Mesima Basin (Figs 8e, 8f and 9). Both positions, in areas of high 1659–1783 σ_f drop, are problematic, which highlights either the difficulty of deriving locations from macroseismic effects in areas where, 8 yr later, people still lived in wooden huts in the wake of the 1783 disaster, or uncertainties in the rupture parameters assigned to events prior 1791.

The 1905 September 8, $M \sim 7$, 'Pizzo' earthquake, which was strongly felt throughout Calabria and caused extensive damage in the region between Capo Vaticano and southwestern Sila (Fig. 1), also seems to have ruptured a fault in an area of 1783 σ_f decrease. The spread of major isoseismals inland and the observed tsunami imply an offshore location at a depth greater than 10 km. However, both macroseismic (e.g. Baratta 1906; Mercalli 1906; Boschi *et al.* 1995) and instrumental data (Cello *et al.* 1982) show ambiguity on its epicentral location and hypocentral depth. Besides, its focal mechanism (Cello *et al.* 1982), inconsistent with the regional stress field, suggests that it occurred on a radically different fault system, still too poorly understood to be included in any form of modelling.

The last large event, on the other hand, the $M_w = 7.1$, 1908 December 28 Messina earthquake ruptured a fault in the Messina Strait, fully within a zone of high 1783 σ_f rise, reaching ~ 2 bar (Figs 8e and f). The focal mechanism, consistent with north-trending, oblique normal faulting (Fig. 1), is compatible with optimal fault orientations predicted by the Coulomb modelling (Figs 8e and f). Such results are strengthened by adding the effects of the large 1693 January 11 southeast Sicily earthquake ($I_{max} >$ XI, $M = 7$–7.5) into the modelling. The fault responsible for this earthquake (Bianca *et al.* 1997) appears to be located offshore in the Ionian Sea southeast of Mount Etna (Fig. 1; F4 of Hirn *et al.* 1997). Assuming a magnitude of ~ 7.2, corresponding to a seismic moment of $\sim 7 \times 10^{19}$ N m, and a ~ 45 km long dextral normal fault rupture, consistent with WNW–ESE regional extension, would increase the $\Delta\sigma_f$ in the Messina Strait (Fig. 9), near the epicentral location of the 1908 Messina earthquake, by ~ 2.5 bar.

SUMMARY AND CONCLUSIONS

Our study of the 1783 seismic sequence and associated faults provides new, self-consistent information on current regional tectonics, seismogenic faulting, source parameters and stress triggering of large earthquakes in Calabria and Sicily. Historical chronicles and geomorphological observations concur to indicate that four of the main shocks of 1783 were undoubtedly shallow (≤ 20 km) and due to slip on the normal 60°–70°W-dipping Galatro–Cittanova–Sant'Eufemia faults (February 5 event), Scilla Fault (February 6 event) and Serre Fault (February 7 and March 1 events). Together, these stepping faults bound the 100 km long western edge of Calabria's mountainous backbone (Serre and Aspromonte), with steep cumulative escarpments up to 400–500 m high, and uplifted Pleistocene marine terraces on their footwalls reflecting minimum throw rates of 0.5–1 mm yr^{-1}.

Analysis of the time sequence of and elastic stress coupling between the 1783 and other events, by resolving the Coulomb failure stress changes ($\Delta\sigma_f$) on faults with given strikes or optimally oriented within the regional stress field ($\sim$N125°E extension), strengthens the interpretation that the faults belong to a single, large-scale tectonic system. The first and largest earthquake (1783 February 5, $M \sim 7$), which ruptured 'simultaneously' the Cittanova, Sant'Eufemia and Galatro faults, triggered the second, 1783 February 6 earthquake ($M \sim 6.3$) on the Scilla Fault by increasing σ_f by 5–10 bar. By increasing σ_f by $>$ 1–5 bar, these two shocks subsequently triggered the 1783 February 7 shock ($M \sim 6.5$) on the Serre Fault. The combined effects of the first three events increased σ_f by about 1 bar further north on the same fault, triggering the 1783 March 1 shock ($M \sim 5.7$). The gap between the 1783 February 7 and 1783 March 1 ruptures appears to result from a centennially persistent stress release due to previous rupture of the Serre Fault by the 1659 November 5 ($M \sim 6$) earthquake. The modelling does not explain as clearly the triggering of the last event of the 1783 sequence (March 28) and fails altogether to account for the occurrences of the 1791 and 1905 earthquakes. Such failure, however, may be related to the fact that the locations, depths and tectonic settings of all three events are unclear. This notwithstanding, the final implication of our modelling is that the ~ 2.5 bar σ_f increase resulting from the entire 1783 Calabria sequence and the 1693 SE Sicily earthquake triggered the disastrous 1908 Messina earthquake.

Over a period of about 250 yr (1659–1908), therefore, almost the whole 200 km length of the Siculo-Calabrian rift zone (Tapponnier *et al.* 1987; Tortorici *et al.* 1995; Monaco *et al.* 1997) ruptured, through normal faulting $M \sim 7$ earthquakes and associated sequences of $M \sim 5.5$–6.5 shocks. This confirms that the large earthquakes that strike southern Italy are related to a process—transverse Quaternary rifting—radically different from the subduction regime that presided until the end of the Pliocene. Only one area appears to be characterized by the occurrence of much more frequent, smaller shocks, the Timpe normal fault zone at the foot of Mount Etna (Monaco *et al.* 1997). This is possibly due to the different thermal structure of the crust, which, in the vicinity of this large, permanently active rift volcano, should be hotter and thus weaker. Only one very large earthquake prior to 1650 is recorded in historical chronicles of the region: the 1169 February 4 event, which killed more than 15 000 inhabitants in Catania (Baratta 1901) and was strongly felt in Messina, Reggio and Siracusa ($I =$ X, Boschi *et al.* 1995). Although this event probably ruptured one of the normal faults offshore the eastern coast of Sicily, it is still unclear which. It is also unclear whether this event should be included in a longer ~ 1000 yr sequence of complete stress release or whether it marks the end of a previous sequence. Given the ~ 1 mm yr^{-1} throw rate on the largest faults of the

system, a recurrence time of 2000 yr might be expected for events comparable to those of 1783 February 5, 1693 January 11 or 1908 December 28. If the overall stretching rate across the extensional belt were greater (e.g. $\sim$2 mm yr^{-1}), however, or varied along strike, the return time of large events might locally be shorter (e.g. $\sim$1000 yr).

Be that as it may, the present study provides one convincing example where the use of Coulomb stress modelling brings fruitful insight into the spatial dynamics of seismic sequences for which individual events are adequately located, even when they occurred before the instrumental period, and the corresponding faults and slip styles correctly identified. Such modelling thus proves to be a powerful tool to assess long-term earthquake hazard in tectonically active regions, as recently demonstrated in other parts of the Mediterranean, such as western Turkey (Stein *et al*. 1997; Hubert *et al*. 2000; Parsons *et al*. 2000).

ACKNOWLEDGMENTS

We thank G. C. P. King, L. Dorbath and an anonymous referee for constructive comments. Financial support was provided by the Programme National des Risques Naturels, INSU Contribution No. 295, CNRS and Program Faust (project ENVA4 CT 970528) from the EEC. This is IPG Paris contribution No. 1750.

REFERENCES

Amato, A., Azzara, R., Basili, A., Chiarabba, C., Cocco, M., Di Bona, M. & Selvaggi, G., 1995. Main shock and aftershocks of the December 13, 1990 Eastern Sicily earthquake, *Ann. Geofis.,* **38,** 255–266.

Anderson, H. & Jackson, J., 1987. The deep seismicity of the Tyrrhenian Sea, *Geophys. J. R. astr. Soc.,* **91,** 613–637.

Armijo, R., Dechamps, A. & Poirier, J.P., 1986. *Carte Sismotectonique de l'Europe et Du Bassin Mediterraneen,* IPGP, Institut Géographique National, Paris.

Baratta, M., 1901. *I Terremoti d'Italia,* Arnoldo Forni, Torino.

Barratta, M., 1906. Il grande terremoto Calabro dell'8 Settembre 1905, *Atti Della Società Toscana Di Sciencze Naturali Di Pisa, Memorie,* **22,** 57–80.

Barrier, P., 1987. Stratigraphie de dépôts pliocènes et quaternaires du Détroit de Messine, *Doc. Trav. IGAL, Paris,* **11,** 59–81.

Barrier, P. & Keraudren, B., 1983. Mise en évidence d'un passage stratigraphique continu entre une terrasse tyrrhénienne de la région de Reggio de Calabria et un faciès conglomératique de comblement du Détroit de Messine (Italie), *C. R. Acad. Sci. Paris,* **296,** 1667–1670.

Bassinot, F.C., Labeyrie, L.D., Vincent, E., Quidelleur, X., Shackleton, N.J. & Lancelot, Y., 1994. The astronomical theory of climate and the age of the Brunhes-Matuyama magnetic reversal, *Earth planet. Sci. Lett.,* **126,** 91–108.

Bianca, M., Monaco, C., Tortorici, L. & Cernobori, L., 1997. Active tectonics in eastern Sicily: the 1693 Hyblean earthquakes, *Terra Nova,* **9**, Abstract Suppl. 1, 305–306.

Boccaletti, M., Guazzone, G. & Manetti, P., 1974. Evoluzione paleogeogrfica e geodinamica del Mediterraneo: i bacini marginali, *Mem. Soc. Geol. It.,* **13,** 1–39.

Bonfiglio, L. & Berdar, A., 1986. Gli elefanti del Pleistocene superiore di Archi (RC): nuove evidenze di insularità della Calabria meridionale durante il ciclo Tirreniano, *Boll. Soc. Paleont. It.,* **25,** 9–34.

Boschi, E., Ferrari, G., Gasperini, P., Guidoboni, E., Smriglio, G. & Valensise, G., 1995. *Catalogo Dei Forti Terremoti in Italia Dal 461 A.C. Al 1980,* Istituto Nazionale di Geofisica, S.G.A., Roma.

Bottari, A., Capuano, P., De Natale, G., Gasparini, P., Neri, G., Pingue, F. & Scarpa, R., 1989. Source parameters of earthquakes in the Strait of Messina, Italy, during this century, *Tectonophysics,* **166,** 221–234.

Cello, G., Guerra, I., Tortorici, L., Turco, E. & Scarpa, R., 1982. Geometry of the neotectonic stress field in southern Italy: geological and seismological evidence, *J. struct. Geol.,* **4,** 385–393.

Cotecchia, V., Travaglini, G. & Melidoro, G., 1969. I movimenti franosi e gli sconvolgimenti della rete idrografica prodotti in Calabria dal terremoto del 1783, *Geol. appl. Idrogeol.,* **4,** 1–24.

Dewey, J.F., Helman, M.L., Turco, E., Hutton, D.H.W. & Knott, S.D., 1989. Kinematics of the western Mediterranean, in *Alpine Tectonics,* eds Coward, M.P., Dietrich, D. & Park, R.G., *Geol. Soc. Lond. Spec. Publ.*, 45, 265–283.

Dolomieu, D., 1784. *Mémoire sur les Tremblemens de Terre de la Calabre Pendant l'Année 1783,* Fulgoni, Rome.

Dumas, B., Gueremy, P., Lhenaff, R. & Raffy, J., 1979. Relief et néotectonique de la façade orientale du Détroit de Messine (calabre, Italie), *Trav. RCP CNRS,* **461,** 95–125.

Dumas, B., Gueremy, P., Lhenaff, R. & Raffy, J., 1980. Terrasses quaternaires soulevées sur la façade calabraise du Détroit de Messine (Italie), *C. R. Acad. Sci. Paris,* **290,** 739–742.

Dumas, B., Gueremy, P., Lhenaff, R. & Raffy, J., 1982. Le soulèvement quaternaire de la Calabre méridionale, *Rev. Géol. Dyn. Géogr. Phys.,* **23,** 27–40.

Gasparini, C., Iannaccone, G., Scandone, P. & Scarpa, R., 1982. Seismotectonics of the Calabrian Arc, *Tectonophysics,* **84,** 267–286.

Ghisetti, F., 1981. Upper Pliocene-Pleistocene uplift rates as indicators of neotectonic pattern: an example from southern Calabria (Italy), *Z. Geomorph. NF Suppl.,* **40,** 93–118.

Ghisetti, F. & Vezzani, L., 1982. The recent deformation mechanisms of the Calabrian Arc, *Earth Evol. Sci.,* **3,** 197–206.

Gignoux, M., 1913. Les formations marine pliocènes et quaternaires de l'Italie du Sud et de la Sicilie, *Ann. Univ. Lyon,* **36,** 1–369.

Hamilton, W., 1783. *An Account of Earthquakes in Sicily and Calabria,* Royal Society, London.

Hippolyte, J.C. & Bouillin, J.P., 1999. Morphologie et cinématique d'une faille holocène dans les monts Péloritains (Sicile); implication géodynamique, *C. R. Acad. Sci. Paris,* **329,** 741–747.

Hirn, A. *et al.*, 1997. Roots of Etna volcano in faults of great earthquakes, *Earth planet. Sci. Lett.,* **148,** 171–191.

Hubert-Ferrari, A., Barkat, A., Jacques, E., Nalbant, S.S., Meyer, B., Armijo, R., Tapponnier, P. & King, G.C.P., 2000. Seismic hazard in the Marmara Sea following the 17 August 1999 Izmit earthquake, *Nature,* **404,** 269–272.

Jacques, E., 1995. Fonctionnement sismique et couplage élastique des failles en Afar, *PhD thesis,* Université de Paris VII, IPGP, Paris.

Jacques, E., King, G.C.P., Tapponnier, P., Ruegg, J.C. & Manighetti, I., 1996. Seismic activity triggered by the 1978 events in the Asal Rift, Djibouti, *Geophys. Res. Lett.,* **23,** 2481–2484.

Kanamori, H., 1977. The energy release in great earthquakes, *J. geophys. Res.,* **82,** 2981–2987.

King, G.C.P., Stein, R.S. & Rundle, J.B., 1988. The growth of geological structures by repeated earthquakes 1, Conceptual framework, *J. geophys. Res.,* **93,** 13 307–13 318.

King, G.C.P., Stein, R.S. & Lin, J., 1994. Static stress changes and the triggering of earthquakes, *Bull. seism. Soc. Am.,* **84,** 935–953.

Malinverno, A. & Ryan, W.B.F., 1986. Extension in the Tyrrhenian Sea and shortening in the Apennines as result of arc migration driven by sinking of the lithosphere, *Tectonics,* **5,** 227–245.

Manighetti, I., Tapponnier, P., Courtillot, V., Gallet, Y., Jacques, E. & Gillot, P.Y., 2001a. Strain transfer between disconnected, propagating rifts in Afar, *J. geophys. Res.,* **106,** 13 613–13 665.

Manighetti, I., King, G.C.P., Gaudemer, Y., Scholz, C. & Doubre, C., 2001b. Slip accumulation and lateral propagation of active normal faults in Afar, *J. geophys. Res.,* **106,** 13 667–13 696.

Mazzuoli, R., Tortorici, L. & Ventura, G., 1995. Oblique rifting in Salina, Lipari and Vulcano islands (Aeolian Islands, Southern Italy), *Terra Nova,* **7,** 444–452.

Mercalli, G., 1906. Alcuni risultati ottenuti dallo studio del terromoto calabrese dell'8 settembre 1905, *Atti Dell'Academica Pontaniana,* **36,** 1–9.

Monaco, C., Petronio, L. & Romanelli, M., 1995. Tettonica estensionale nel settore orientale del Monte Etna (Sicilia), *Studi Geologici Camerti,* **2,** 363–374.

Monaco, C., Tortorici, L., Nicolich, R., Cernobori, L. & Costa, M., 1996. From collisional to rifted basins: an example from the southern Calabrian arc (Italy), *Tectonophysics,* **266,** 233–249.

Monaco, C., Tapponnier, P., Tortorici, L. & Gillot, P.Y., 1997. Late Quaternary slip rates on the Acireale Piedimonte normal faults and tectonic origin of Mt. Etna (Sicily), *Earth planet. Sci. Lett.,* **147,** 125–139.

Nostro, C., Cocco, M. & Belardinelli, M.E., 1997. Static stress changes in extensional regimes: an application to southern Apennines (Italy), *Bull. seism. Soc. Am.,* **87,** 234–248.

Ogniben, L., 1973. Schema geologico della Calabria, in base ai dati odierni, *Geol. Romana,* **12,** 243–585.

Parson, T., Toda, S., Stein, R.S., Barka, A. & Dieterich, J.H., 2000. Heightened odds of large earthquakes near Istanbul: an interaction-based probability calculation, *Science,* **288,** 661–665.

Postpischl, D., 1985. *Catalogo Dei Terremoti Italiani Dall'anno 1000 Al 1980,* CNR, PF Geodinamica, Graficcop, Bologna.

Reasenberg, P.A. & Simpson, R.W., 1992. Response of regional seismicity to the static stress change produced by the Loma Prieta earthquake, *Science,* **255,** 1687–1690.

Rehault, J.P., Boillot, G. & Mauffret, A., 1984. The Western Mediterranean basin geological evolution, *Mar. Geol.,* **55,** 447–477.

Sarconi, M., 1784. *Istoria de' fenomeni del tremuoto avvenuto nelle Calabrie, e nel Valdemone nell'anno 1783 posta in luce dalla Reale Accademia delle Scienze, e delle Belle Lettere di Napoli,* Napoli.

Scholz, C.H., 1990. *The Mechanics of Earthquakes and Faulting,* Cambridge University Press, Cambridge.

Stein, R.S., King, G.C.P. & Lin, J., 1992. Change in failure stress on the southern San Andreas fault system caused by the 1992 magnitude = 7.4 Landers earthquake, *Science,* **258,** 1328–1332.

Stein, R.S., Barka, A.A. & Dieterich, J.H., 1997. Progressive failure on the North Anatolian fault since 1939 by earthquake stress triggering, *Geophys. J. Int.,* **128,** 594–604.

Tapponnier, P., 1977. Evolution tectonique du système alpin en Méditerranée: poinçonnement et écrasement rigide-plastique, *Bull. Soc. Géol. Fr.,* **19,** 437–460.

Tapponnier, P., Tortorici, L. & Winter, T., 1987. Faulting during the 1783 Calabria Earthquakes and tectonics of the Messina Strait, *Terra Abstract, Terra Cognita,* 305.

Tortorici, L., Monaco, C., Tansi, C. & Cocina, O., 1995. Recent and active tectonics in the Calabrian Arc (Southern Italy), *Tectonophysics,* **243,** 37–55.

Valensise, G. & Pantosti, D., 1992. A 125 kyr-long geological record of seismic source repeatability: the Messina Straits (southern Italy) and the 1908 earthquake (M 7, 1/2), *Terra Nova,* **4,** 472–483.

Vivenzio, G., 1783. *Istoria e Teoria dei Tremuoti in Generale ed in Particolare di Quelli della Calabria e di Messina del 1783,* Stamperia Regale, Napoli.

Wells, D.L. & Coppersmith, K.J., 1994. New empirical relationships among magnitude, rupture length, rupture width, rupture area and surface displacement, *Bull. seism. Soc. Am.,* **84,** 974–1002.

Westaway, R., 1993. Quaternary uplift of Southern Italy, *J. geophys. Res.,* **98,** 21 741–21 722.